©2011 Society of Economic Geologists, Inc.
Economic Geology, v. 106, pp. 945–973

Hydrothermal Alteration and Veins at the Epithermal Au-Ag Deposits and Prospects of the Waitekauri Area, Hauraki Goldfield, New Zealand

Mark P. Simpson† and Jeffrey L. Mauk

School of Environment, The University of Auckland, Private Bag 92019, Auckland, New Zealand

Abstract

The Waitekauri area of the Hauraki goldfield, New Zealand, contains several adularia-sericite epithermal Au-Ag deposits and prospects. From west to east, the area contains the Sovereign, Jubilee, Scimitar, Scotia, Teutonic, and Jasper Creek deposits and prospects, which are hosted by andesitic and dacitic flows, breccias, and localized pyroclastic and air fall deposits. Drill core reveals spatial and temporal zonation of alteration and vein minerals along a 3-km-long composite cross section through the area. Most host rocks are intensely altered, with 100 percent of the igneous minerals replaced by hydrothermal minerals, although the alteration intensity becomes more variable and weaker toward the east. Alteration minerals include quartz, adularia, albite, chlorite, pyrite, illite, interstratified illite-smectite, smectite, calcite, hematite, and minor epidote. Many of these minerals have zoned distributions; adularia is widespread at Sovereign, but is restricted to shallow levels at both Scotia and Jasper Creek. Albite occurs in a discrete zone below adularia at Scotia, and minor epidote is restricted to Sovereign and Jubilee. Illite occurs throughout Sovereign and Jubilee and at the western margin of Scotia and Scimitar, where it grades eastward into interstratified illite-smectite and smectite at Teutonic and Jasper Creek. Veins are typically less than 10 cm wide, but have diverse mineralogy with zoned distributions. Quartz veins dominate at Sovereign and Jubilee, whereas calcite veins are more abundant at Scotia, Scimitar, and Jasper Creek. Laumontite occurs at Scotia and locally at Scimitar, whereas veins of clinoptilolite and mordenite ± calcite occur at Jasper Creek and stilbite veins occur at Teutonic.

Fluid inclusions in quartz and calcite homogenized between 132º and 310ºC and trapped a dilute solution with an apparent salinity of less than 2.6 wt percent NaCl equiv. Homogenization temperatures are highest at Sovereign (avg. 241ºC), Jubilee (avg 239ºC), and Scimitar (avg 236ºC), lower at Scotia (avg 204ºC) and lowest at Teutonic (avg 168 ºC) and Jasper Creek (avg 162ºC). Estimated positions of the paleowater table above Sovereign, Jubilee, Scimitar, Scotia, Jasper Creekg and Teutonic relative to present elevations was at least 690, 750, 575, 450, 225, and 150 m above sea level, respectively; the deposits and prospects, therefore, span a 600-m vertical interval. Individual deposits and prospects have undergoen at least 35 to more than 455 m of erosion with the greatest erosion to the west.

Alteration intensity, alteration and vein mineral distributions, and fluid inclusion microthermometry are interpreted to indicate that Sovereign and Jubilee formed at relatively high temperatures, whereas Teutonic and Jasper Creek formed at relatively cooler temperatures. Several hydrologic reconstructions are possible, including (1) a single hydrothermal system with an inclined water table and significant lateral outflow to the east, or 2) a single low-relief hydrothermal system with a flat-lying water table that has subsequently been displaced by postmineral faults or tilted approximately 10º to the east. Regardless of the preferred reconstruction, the Sovereign and Jubilee deposits appear to have formed in the main zone of fluid upflow, whereas the Teutonic and Jasper Creek prospects appear to have formed toward the margin. Moreover, the greatest erosion has occurred at the Jubilee and Sovereign deposits (~300–400 m), and these may represent the roots of a more extensive vein network that has largely been eroded.

Introduction

Gold and silver in adularia-sericite epithermal deposits typically occur in structurally controlled veins that are mineralized over a relatively confined vertical extent and are enveloped by extensive zones of hydrothermal alteration that may extend over tens, hundreds, or thousands of meters (e.g., Mule Canyon, Nevada: John et al., 2003; Comstock: Hudson, 2003; Favona, New Zealand: Simpson and Mauk, 2007). Many papers describe alteration in terms of general mineral associations that have been adopted from terminology used to describe alteration of porphyry Cu deposits (i.e., potassic, argillic, propylitic), whereas others describe the distribution of individual alteration minerals and vein types (e.g., Conrad et al., 1992; Hudson, 2003; Simpson and Mauk, 2007). Although the former method is very useful for field mapping, the recognition and delineation of associations is complicated by overlapping mineralogy and does not take into account the formation of different minerals at different times. In geothermal fields, the active analogues of some epithermal deposits, the distributions of individual alteration minerals are routinely determined during drilling to assess reservoir temperature, inferred permeability, and fluid compositions that are only directly measurable following drilling and well testing (e.g., Henley and Ellis, 1983; Reyes, 1990; Simmons and Browne, 2000; Mas et al., 2006). Here, we describe the geologic setting, hydrothermal alteration, and vein types at the volcanic rock-hosted epithermal Au-Ag deposits and prospects in the Waitekauri area of the southern Hauraki goldfield, North Island, New Zealand (Figs. 1, 2). The area has been well drilled, and we present alteration and vein mineralogy and fluid inclusion data along three cross sections that total 3 km in length; these sections range from the center to the margin of the hydrothermally altered area, and provide a 600-m reconstructed vertical range of the Waitekauri deposits

† Corresponding author: e-mail, ma.simpson@auckland.ac.nz

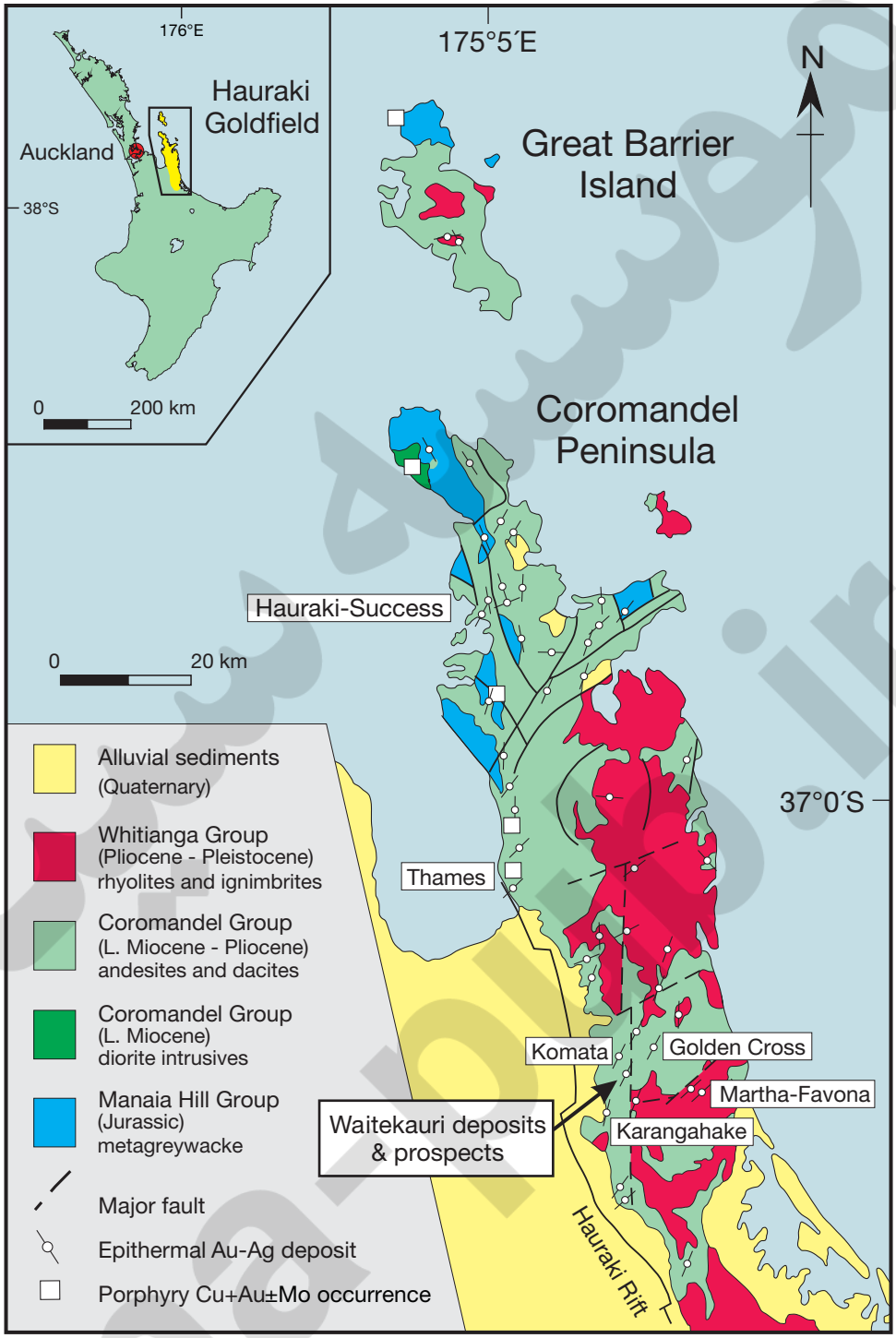

FIG. 1. Geologic map of the Coromandel peninsula showing the location of the Waitekauri deposits and prospects plus other significant deposits (Skinner, 1986; Christie et al., 2007).

and prospects. Booden et al. (2011) further document the geochemistry of hydrothermal alteration along these sections. We use alteration, vein, and fluid inclusion data to interpret the physical and chemical conditions that prevailed during hydrothermal activity, which allows us to infer the nature of the hydrothermal system(s) that formed these deposits and prospects.

Regional Geology

The Waitekauri deposits and prospects occur in the southern part of the Hauraki goldfield (Fig. 1), a 200-km-long by 40-km-wide metallogenic province that contains approximately 50 epithermal Au-Ag deposits and several porphyry Cu-Au-Mo occurrences (Christie et al., 2007). Deposits are hosted in a Miocene to Pliocene continental margin volcanic

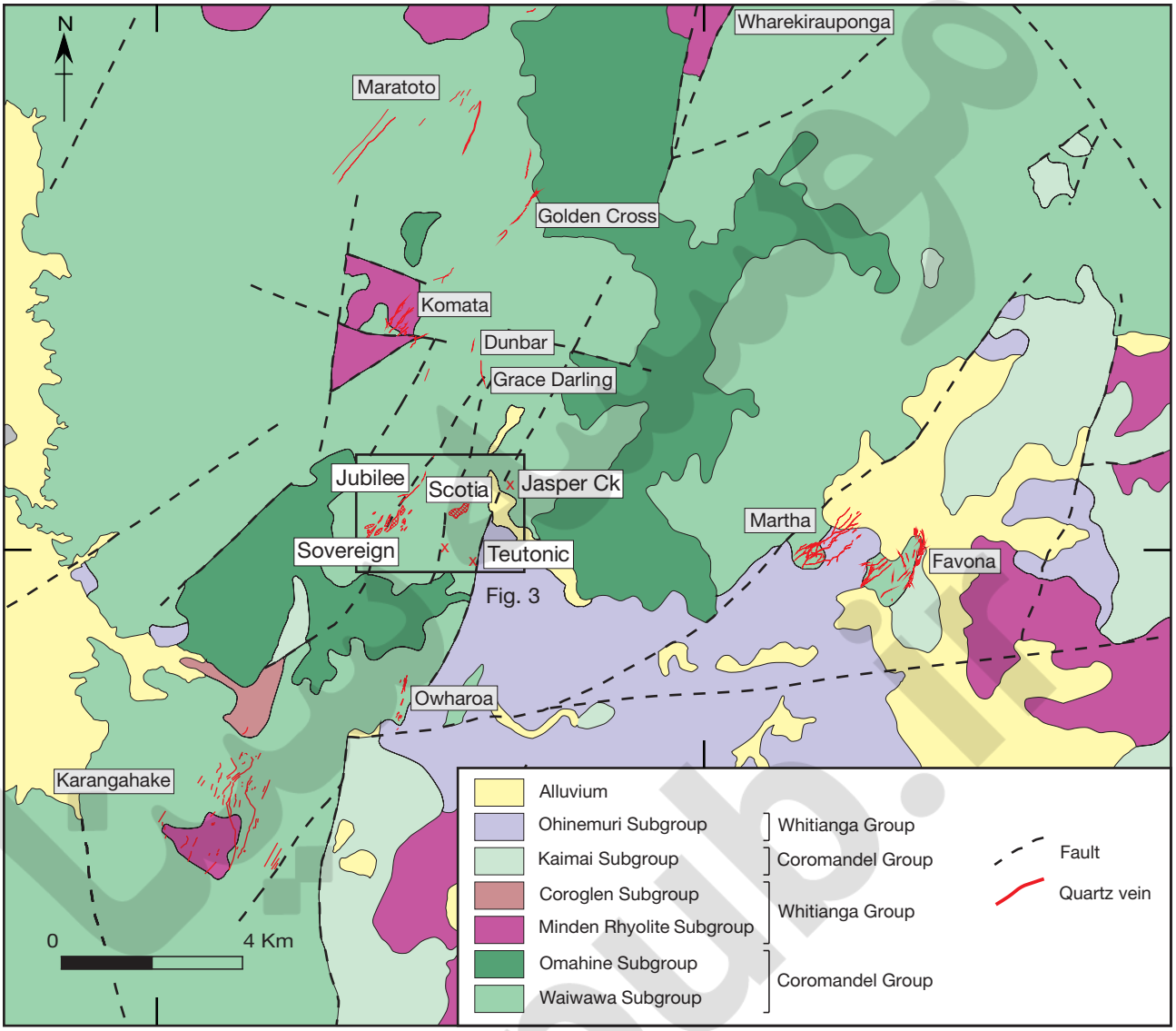

FIG. 2. Regional geologic map of the southern Coromandel peninsula, showing the location of the Waitekauri deposits and prospects, which includes the Sovereign, Jubilee, and Scotia deposits, and the Scimitar, Teutonic, and Jasper Creek prospects. Redrawn from Brathwaite and Christie (1996) and unpublished Newmont Waihi operations maps. Other epithermal Au-Ag deposits in the area include Golden Cross (~0.75 Moz Au), Karangahake (~0.95 Moz Au), Martha (>6.7 Moz Au), and Favona (>0.6 Moz Au) (Christie et al., 2007).

arc, the subaerial sector of the Coromandel volcanic zone that formed due to convergence along the Pacific-Australian plate boundary (Nicholson et al., 2004; Mortimer et al., 2007). Basement rocks consist of Late Jurassic graywacke and argillites of the Manaia Hill Group that are unconformably overlain by Miocene to Pliocene (ca. 18–4 Ma) andesitic and dacitic flows and volcaniclastic rocks of the Coromandel Group (Skinner, 1986, 1995; Adams et al., 1994). These groups are intruded by subvolcanic dikes and rare quartz diorite to granodiorite stocks with locally associated porphyry Cu-Au-Mo mineralization (Brathwaite et al., 2001a). Late Miocene to Pliocene (ca. 11–1.9 Ma) rhyolitic flows and pyroclastic rocks of the Whitianga Group form several caldera complexes with eruptive products that interfinger with and overlie the Coromandel Group andesite (Skinner, 1986; Adams et al., 1994). Farther south, the volcanic rocks of the Coromandel volcanic zone merge with and are overlain by Quaternary (2.0 Ma to present) volcanic rocks of the Taupo volcanic zone (Houghton et al., 1995; Briggs et al., 2005).

The Hauraki goldfield is cut by north-northwest– and north-northeast– to east-northeast–striking faults (Skinner, 1986). North-northwest–striking faults displace rocks downward to the east and west, whereas most north-northeast– to east-northeast–striking faults displace rocks downward to the south; this results in increased exposure of the graywacke basement in the north, and thicker exposures of volcanic rocks to the south (Fig. 1).

Epithermal deposits are hosted in andesite, dacite, rhyolite, and graywacke (Figs. 1, 2), with more than 96 percent of all Au extracted from quartz veins hosted in andesite and dacite

(Christie et al., 2007). Veins are steeply dipping, vary from 300 to 1,300 m in length, are 1 to 5 m wide, and most were mined over vertical intervals of 170 to 330 m, although many continued at depth with low Au and Ag content (e.g., Golden Cross; Simpson et al., 2001). Total production from 1862 through 2009 was 334,600 kg Au and 1.56 Mkg Ag (Christie et al., 2007, updated with 2006–2009 production figures from Newmont Waihi Gold).

Local Geology

Gold was discovered at Jubilee Hill at the Old Waitekauri claim by Daniel Leahy in 1875 (Bell and Fraser, 1912); this was followed by additional discoveries at nearby Owharoa, Grace Darling, Durbar, Komata, Golden Cross, Maratoto, and neighboring Karangahake and Waihi (Martha) deposits (Fig. 2). The Waitekauri area includes the Sovereign, Jubilee, and Scotia deposits, which produced 37,090 oz Au-Ag bullion from intermittent mining between 1875 and 1929 (Downey, 1935), and the recently explored Jasper Creek, Scimitar, and Teutonic prospects (Figs. 2, 3). Renewed exploration began in 1978 following a regional aeromagnetic survey by Amoco Minerals NZ Ltd that identified targets in the area. Between 1980 and 1996, exploration by Cyprus Minerals (formerly Amoco), and Coeur Gold NZ Ltd included geologic mapping, soil, outcrop, and adit sampling, resistivity surveys and 87 drill holes (10,605 m). Best drill intercepts include 11 m @ 3.34 g Au/t at Sovereign and 10.2 m @ 6.04 g Au/t at Scotia. Continuous chip sampling in an adit at Scotia also returned 5 m @ 11.87 g Au/t (McOnie, 2001). The area was more recently explored from 2004 to 2008, by Welcome Gold NZ Ltd, and tested by 19 drill holes (6,830 m).

The Waitekauri deposits and prospects are hosted by andesitic and dacitic flows, breccias, and pyroclastics of the Waipupu Formation, Mangakara Dacite, and Waitekauri Dacite, which are intruded by dikes of Maratoto Rhyolite (Fig. 3). These are unconformably overlain by postmineral Whakamoehau Andesite and Owharoa Ignimbrite (Brathwaite and Christie, 1996).

The Waipupu Formation (ca. 7.9–6.7 Ma) consists of two-pyroxene andesitic lava flows, lesser volcanic breccias and localized intercalations of lithic-crystal tuffs, and minor epiclastic sedimentary rocks (Brathwaite and Christie, 1996). This unit is the most important host rock at Jubilee and Jasper Creek; it occurs at depth below Scotia and Scimitar, and it is common at Sovereign (Fig. 3). The Mangakara Dacite (ca. 6.90 Ma) overlies or is in fault contact with the Waipupu Formation and consists of pyroxene-hornblende dacite and rhyodacite flows that occur at and near the Teutonic and Scimitar prospects (Fig. 3; Haworth and Briggs, 2006). The Waitekauri Dacite consists of xenolithic two-pyroxene dacitic lava flows with local tuff breccias and lithic-crystal tuffs; it overlies the Mangakara Dacite (Brathwaite and Christie, 1996; Haworth and Briggs, 2006). At Scotia, the Waitekauri Dacite mostly consists of lava flows, whereas at Sovereign it is dominated by lithic tuffs, tuff breccias, breccias, and minor lava flows (Fig. 3). Some breccias may be either intrusive or hydrothermal, but intense alteration precludes genetic determination (McConnochie, pers. commun., 2006). Northeast-trending dikes of Maratoto Rhyolite that are up to 720 m in length and 1 to 15 m in width intrude Waipupu Formation andesite and Waitekauri Dacite at Jubilee and Sovereign (Brathwaite and Christie, 1996; Haworth and Briggs, 2006). There are also rare andesite dikes and drill hole WV016 contains a 2-m-wide intensely altered dike of coarse-grained quartz diorite. Postmineral andesite to dacite lava flows of Whakamoehau Andesite (ca. 6.70–6.61 Ma) unconformably overlie all the above units, and the area east of Teutonic is blanketed by Owharoa Ignimbrite (ca. 3.69 ± 0.06 Ma; Hoskin et al., 1998).

Veins occur in, or are separated by, a series of north-northeast–striking normal faults that include the Waitekauri, Tunnel, Grace Darling, and Owharoa faults (Fig. 3); these faults dip east-southeast, except for the Waitekauri fault, which dips west-northwest (Haworth and Briggs, 2006). The most important structures controlling mineralization are the Waitekauri and Tunnel faults (Fig. 3). The Jubilee vein and veins at Sovereign occur along the north-northeast–striking and steeply (60°–80°) west-northwest–dipping Waitekauri fault, which at Sovereign further splays into the Realm and Young New Zealand faults (Grodzicki et al., 2007). West- to northwest-striking faults are less common and include the Central and George faults with the former dipping 65° to the south-southwest. All faults display normal displacements, although the amount of offset is not known owing to poor exposures and a lack of marker horizons (Grodzicki et al., 2007).

The main Au-Ag mineralized quartz vein is the north-northeast–trending Jubilee vein that historically produced 28,965 oz Au-Ag bullion from 18,923 t of ore and accounts for 78 percent of production at Waitekauri (Downey, 1935). This vein consists of a single vein at depth that splays into several narrow veins near surface. It has a strike length of 990 m, a vertical extent that exceeds 215 m, and it averages 2.4 m in width, although it is strongly lenticular and commonly narrows to several centimeters (Bell and Fraser, 1912; Downey, 1935). Quartz is typically massive to coarsely crystalline and locally comb, with Au and Ag associated with fine-grained volumetrically minor crustiform banded quartz. Assay results indicate Ag/Au ratios of 1.0 to 1.8 and up to 36.8 g/t Au and 37 g/t Ag, although much of the vein is subeconomic (Hartley and McConnochie, 1991). Base metal sulfide minerals, including sphalerite, galena and chalcopyrite, occur at depth and are associated with up to 318 g/t Ag (Bell and Fraser, 1912; Hartley and McConnochie, 1991). By contrast, quartz veins at Sovereign and Scotia are typically narrow and rarely exceed 1 m in width. At Sovereign, Au and Ag also occur in silicified and fractured breccia zones (Bell and Fraser, 1912; White, 1991). No significant veins or mineralization have been found at Jasper Creek, however, a polymict breccia contains clasts of andesite and rare sinter with relict plant fragments.

Adularia from a quartz vein at the Sovereign deposit yielded $^{40}Ar/^{39}Ar$ plateau, isochron, and total gas dates that overlap within error, and a preferred age of 6.70 ± 0.16 Ma (Mauk et al., 2011).

Sampling and Analytical Techniques

Hydrothermal altered rocks and veins were examined in drill holes along three cross sections that collectively total 3 km in length and transect the (1) Sovereign, Scimitar, Teutonic (6420150m N), (2) Jubilee and Scotia (6420800m N), and (3) Jasper Creek (6421150m N) deposits and prospects (Figs. 3, 4). Cross section numbers refer to the New Zealand

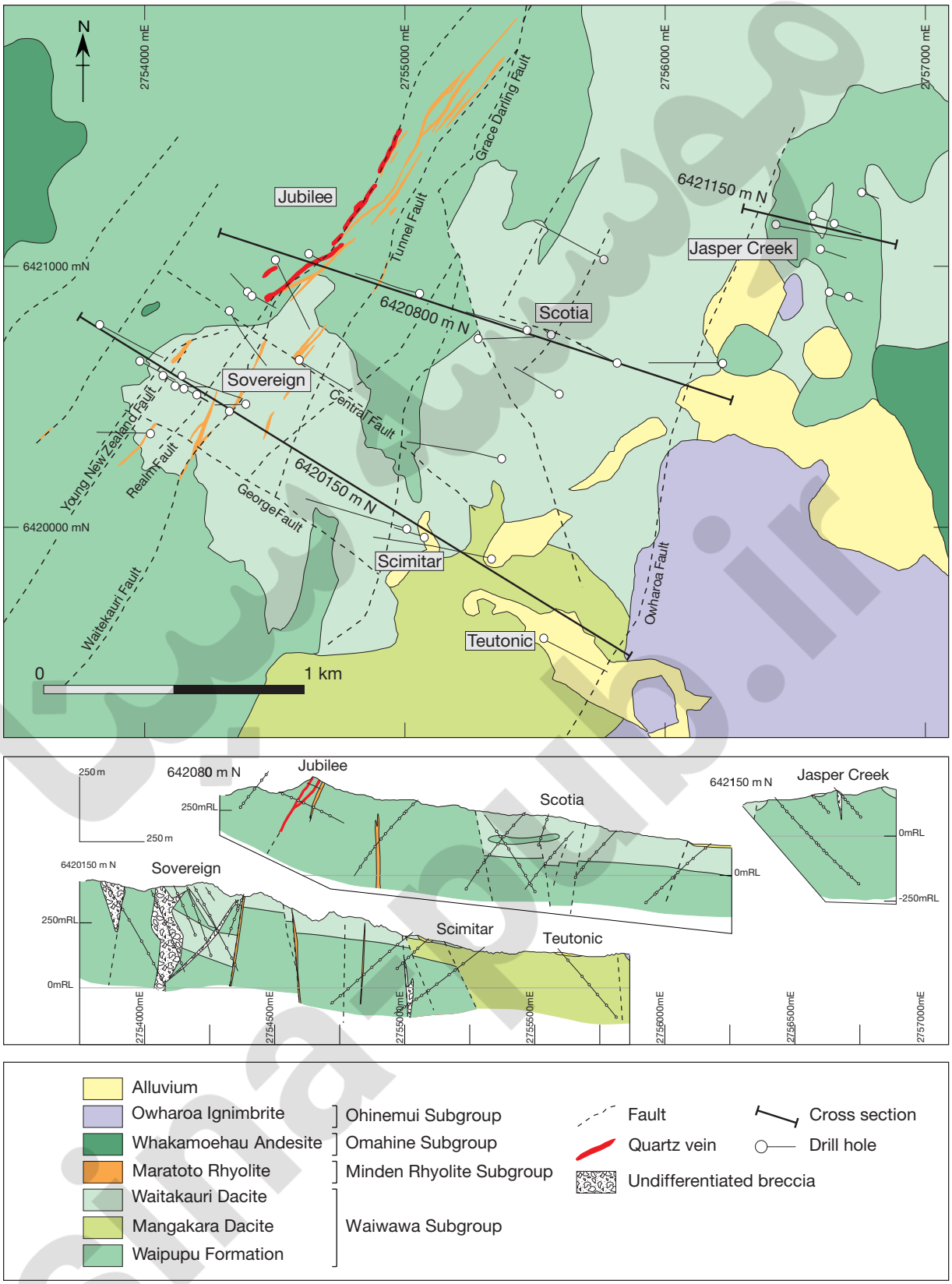

FIG. 3. Surface and cross section geology of the Waitekauri deposits and prospects showing the position of the 6421150m N Jasper Creek, 6420800m N Jubilee-Scotia and 6420150m N Sovereign-Scimitar-Teutonic cross sections (northing coordinates based on cross section midpoints). Several drill holes protrude above the cross section topographic surface because they have been projected onto the section. Redrawn from unpublished Newmont Waihi operations maps.

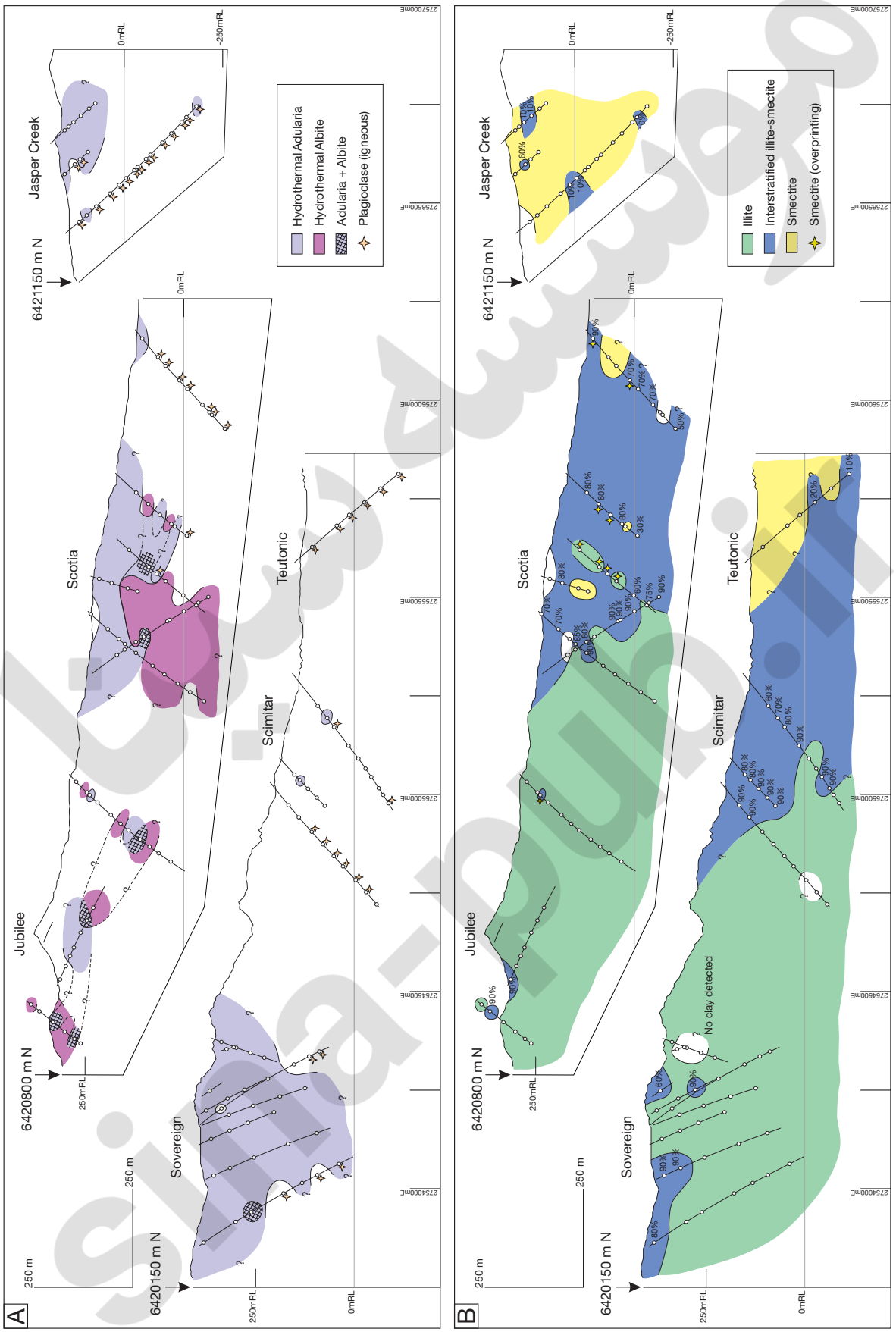

FIG. 4. Cross sections showing the distribution of A) hydrothermal adularia, hydrothermal albite, plus relict igneous plagioclase, and B) illite, interstratified illite-smectite, and smectite. Percentages shown beside samples containing interstratified illite-smectite indicate the amount of illite within these clay minerals. Several samples contain either illite or interstratified illite-smectite that have been overprinted by later smectite; Figure 3 shows cross section locations.

map grid north coordinate at the midpoint of each cross section. Samples were collected from 9,000 m of drill core at 30- to 50-m intervals and selected to represent the intensity and type of hydrothermal alteration, veins and lithology. Hydrothermal alteration minerals have been determined for 225 samples using standard whole-rock and clay-separate X-ray diffraction (XRD) techniques. An additional 33 vein samples were analyzed by XRD to determine zeolite mineralogy. In the clay-separate XRD study, the $\leq 2\,\mu$m clay fraction was extracted and analyzed under air-dried and glycolated conditions. The diffractogram data of Reynolds (1980) and Moore and Reynolds (1997) were used to determine clay mineralogy and degree of interstratification. From this suite of 258 samples, 60 rock and vein samples were examined by thin and polished section petrography.

Fluid inclusion homogenization (T_h) and final ice melting (T_m) temperatures were measured for inclusions in quartz (n = 23) and calcite (n = 22) veins. Measurements were made on doubly polished sections (100–200 μm thick) using a Fluid Inc.-adapted USGS heating and freezing stage. The thermocouple was calibrated at 0.0° and –56.6°C using Syn Flinc fluid inclusion standards, with the data reproducible to ± 2.0°C for homogenization temperatures and ± 0.2°C for final ice melting temperatures.

The stable isotopic compositions of oxygen in vein quartz and of oxygen and carbon in calcite was determined at GNS Science, New Zealand, using standard fluoridation and mass spectrometer techniques (Faure and Brathwaite, 2006). Isotopic ratios are reported in per mil relative to the international standard Vienna Standard Mean Ocean Water (VSMOW) for oxygen isotope ratios and Vienna PeeDee Belemnite (VPDB) for carbon isotope ratios, using conventional delta notation. Oxygen and carbon isotope measurements have reproducibilities of better than ±0.1 per mil.

Hydrothermal Alteration

The regional extent of hydrothermal alteration has been broadly determined from field mapping based on limited outcrops (Brathwaite and Christie, 1996) and from an aeromagnetic survey. The aeromagnetic survey shows that deposits and prospects of the Waitkauri area occur within an irregular elongated magnetic quiet zone that is 22 km² in size and includes the Maratoto, Golden Cross, and Komata deposits (Fig. 2; Morrell et al., 2011). This magnetic quiet zone delineates the area where igneous magnetite has been destroyed by hydrothermal alteration, and it is broadly coincident with a K/Th anomaly of similar size that reflects widespread potassium metasomatism (Booden et al., 2011; Morrell et al., 2011). Even though they occur in the same alteration envelope, the distinct ages of the Maratoto (6.41 ± 0.04 Ma), Golden Cross (6.98 ± 0.11 Ma), Komata (6.06 ± 0.06 Ma), and Sovereign (6.70 ± 0.16 Ma) deposits indicate that these deposits formed at different times, possibly from different hydrothermal systems whose alteration halos overlapped (Mauk et al., 2011).

At the Waitekauri deposits and prospects, hydrothermal alteration of the host volcanic flows, breccias, and pyroclastic rocks as seen from drill core is typically intense, with complete replacement of igneous minerals by hydrothermal minerals (>98–100% replacement). Primary igneous textures in volcanic flows are well preserved; however, textures in breccias at Sovereign are poorly preserved and differentiation between volcanic and possibly intrusive-related or hydrothermal breccias is not possible. The degree of alteration toward the east at Teutonic and Jasper Creek is more variable, and includes areas of strongly, moderately, and weakly altered rocks. In moderately altered rocks, where 20 to 50 percent of the igneous minerals have been replaced, igneous plagioclase and magnetite are partially replaced, whereas augite, hypersthene and groundmass interstitial glass are completely replaced by hydrothermal minerals. In weakly altered rocks, less than 20 percent of the igneous minerals are replaced; augite and hypersthene are partially preserved, whereas igneous plagioclase and magnetite are essentially unaltered. Shallow and surface exposures of volcanic rocks at the deposits and prospects are strongly weathered to iron oxyhydroxide, local jarosite, halloysite, kaolinite, and manganese oxides, with oxidation variably penetrating 20 to 65 m below the ground surface, and locally extending up to 260 m along fracture zones. A variety of alteration minerals occur in the Waitekauri area (Table 1). The occurrence, spatial distribution, and temporal relationships of selected minerals are described below.

Quartz

Quartz is the most abundant replacement mineral, occurring in every sample and typically forming 40 to 60 percent of the rock by volume with slightly lower amounts in moderately and weakly altered rocks. Quartz predominantly replaces glass in the groundmass of volcanic rocks, occurring as fine-grained to microscopic interlocking anhedral grains intergrown with chlorite, illite, or interstratified illite-smectite or smectite and disseminated pyrite. In strongly silicified rocks, quartz also replaces augite, hypersthenes, and, rarely, plagioclase phenocrysts. Quartz is also the most abundant mineral in veins as discussed below.

Hydrothermal adularia and albite

Hydrothermal adularia occurs in 80 percent of samples studied from Sovereign, in more than 45 percent of samples from Jubilee, Scotia, and Jasper Creek, but is essentially absent at Scimitar and Teutonic (Fig. 4A). Adularia at Sovereign occurs at all depths (>350 m vertically), although at Scotia and Jasper Creek, it is restricted to a shallow carapace that is ~180 and ~120 m thick, respectively. By contrast, less common hydrothermal albite prominently occurs in a discrete zone below adularia at Scotia, and patchily coexists with adularia at Scotia and at Jubilee (Fig. 4A).

Hydrothermal adularia and albite are among the earliest formed alteration minerals that preferentially replace plagioclase phenocrysts, laths, and the groundmass (Fig. 5A, B). Adularia and lesser albite make up 1 to 15 percent of the host rocks by volume, but are variably replaced by either illite or interstratified illite-smectite and locally overprinted by late calcite and/or smectite (Fig. 5C). The degree of adularia replacement by illite or interstratified illite-smectite is highly variable and ranges from less than 5 to greater than 95 percent, but typically exceeds 40 percent. It is possible that adularia may have been more extensive at Jubilee and Scimitar. However, if so, it has been completely replaced by illite or interstratified illite-smectite and calcite (Fig. 5D).

TABLE 1. Alteration and Vein Minerals at the Waitekauri Deposits and Prospects

Mineral		Abundance	Origin	Occurrence	Mineral		Abundance	Origin	Occurrence
Silicates					Sulfides and sulfosalts				
Albite	●	M	H	Rx	Argentite	○	R	S	V
Adularia	●	A	H	Rx & V	Chalcopyrite	●	R	H	V
Chlorite	●	A	H	Rx & V	Chalcocite	○	R	S	V
Chalcedony	●	R	H	Rx	Covellite	○	R	S	V
Clinoptilolite	✧	R	H	V	Electrum	○	R	H	V
Corrensite	✧	M	H	Rx	Galena	●	R	H	V
Epidote	✧	R	H	Rx & V	Marcasite	●	R	H	V
Illite	●	A	H	Rx & V	Pyrite	●	A	H	V & Rx
Interlayered Chl-Sm	✧	R	H	Rx	Sphalerite	●	R	H	V
Interstratified I-Sm	●	A	H	Rx & V					
Kaolinite	●	R	S	Rx & V?	Phosphates				
Laumontite	✧	R	H	V	Apatite	●	R	H	Rx
Mordenite	✧	R	H	V					
Prehnite	✧	R	H	V	Oxides				
Smectite	●	A	H	Rx & V	Hematite	●	R	H	Rx & V
Stilbite	✧	R	H	V	Iron oxyhydroxides	●	R	S	Rx & V
Quartz	●	A	H	Rx & V	Leucoxene	●	R	H	Rx
Carbonate									
Calcite	●	A	H	Rx & V					

Data from Bell and Fraser (1912) and this study

Symbols: ● = previously reported and confirmed in present study, ○ = previously reported, unconfirmed in present study, ✧ = newly reported from present study. Abundances: A = abundant (>10%), M = minor (1–10%), R = rare (<1%); Origin: H = hypogene, S = supergene; Occurrence, Rx = host rock, V = veins

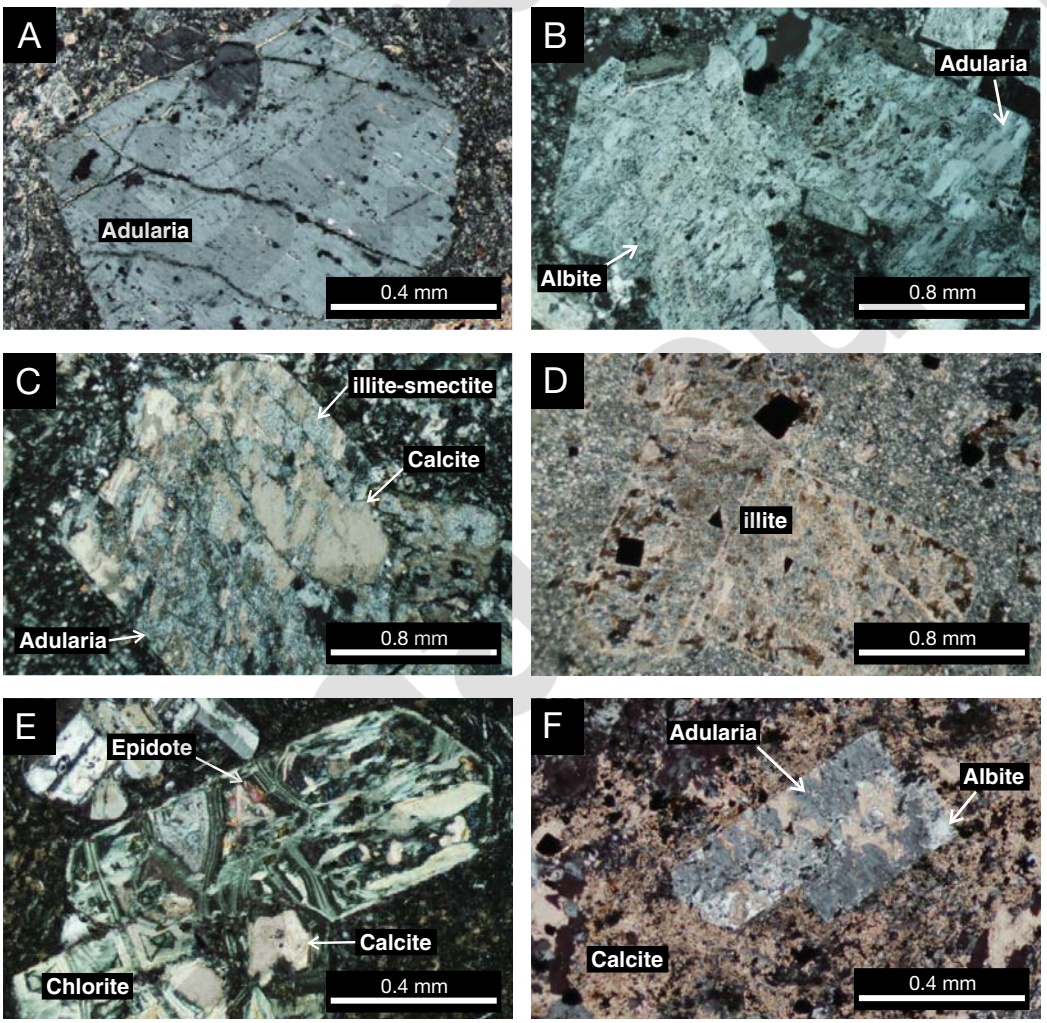

FIG. 5. Images of hydrothermal alteration. A) Plagioclase phenocryst completely replaced by adularia (Sovereign: ML7 36.0 m). B) Plagioclase replaced by hydrothermal albite plus adularia (Jubilee: WV006 254.2 m). C) Hydrothermal adularia partially replaced by interstratified illite-smectite with 80 percent illite and overprinted by later calcite (Scotia: SC28 145.0 m). D) Plagioclase phenocrysts completely replaced by illite plus minor cubic pyrite (Jubilee: WV006 154.5 m). E) Pyroxene phenocryst replaced by chlorite plus minor epidote and calcite (Sovereign: WV001 351.7 m). F) Adularia and albite that have replaced a plagioclase phenocryst and that have been overprinted by late calcite; calcite also has flooded the groundmass (Sovereign: ML13 170.5 m).

Illite, interstratified illite-smectite, and smectite

Illite, interstratified illite-smectite, and smectite are common clay minerals, comprising up to 30 percent of the host rock by volume, and they have zoned distributions from west to east. Illite predominates at Sovereign and Jubilee and on the western margin of Scimitar and Scotia, where it grades eastward into interstratified illite-smectite (Fig. 4B) that contains 10 to 40 percent smectite (Fig. 6). At Teutonic, interstratified illite-smectite with 80 to 90 percent smectite grades into smectite, whereas smectite dominates at Jasper Creek, together with patchy interstratified illite-smectite with 90 percent smectite. In the clay-separate XRD profiles for samples from Jasper Creek and Teutonic, many samples have slightly shifted peak positions suggesting trace amounts of illite (~5%), although definitive identification is beyond the resolution of the technique. All three clay minerals have variably replaced plagioclase, earlier formed hydrothermal adularia and albite (Fig. 5C, D), and they have also flooded the groundmass. Late-stage smectite has locally overgrown interstratified illite-smectite and illite at Scotia.

Chlorite, interlayered chlorite-smectite and corrensite

Chlorite is widespread and occurs in more than 70 percent of samples from Sovereign, Jubilee, Scotia, and Scimitar (Fig. 7A); it is less common at Jasper Creek and Teutonic, where it occurs in 39 and 50 percent of samples, respectively. Chlorite is absent in the deepest drill hole from Jasper Creek and also in several near-surface samples; in the latter locations, due to weathering. In contrast, both corrensite—an ordered, interlayered chlorite-smectite with subequal chlorite and smectite (50:50)—and interlayered chlorite-smectite are rare, and occur in less than 1 and 3 percent of samples, respectively (Fig. 7A). The amount of smectite within interlayered chlorite-smectite is typically indeterminable owing to low peak intensity; however, in more defined profiles this interlayered clay contains 10 to 20 percent smectite.

Petrographic examination reveals that chlorite replaces up to 25 percent of the host rock by volume. It is a significant replacement mineral of the groundmass as well as augite and hypersthene phenocrysts (Fig. 5E). Less commonly, chlorite replaces plagioclase phenocrysts where it occurs along and adjacent to microfractures. Chlorite also fills vesicles, cavities, and rare veins, where it commonly overgrows quartz.

Epidote

Epidote is a volumetrically minor alteration mineral that typically makes up less than 1 percent of the host rock by volume and was only observed during petrographic examination of the samples. Based on a limited number of thin sections (n = 60), epidote occurs in 25 percent of the samples from Sovereign and Jubilee; it was also seen in a single sample from Scimitar (Fig. 7A). The full extent of epidote at Sovereign and Jubilee is not known; it may be more extensive than shown here (Fig. 7A). Epidote replaces phenocrystic plagioclase together with adularia and rare albite, and it is overprinted by late calcite. Together with chlorite, it also replaces mafic phenocrysts (Fig. 5E) and is a rare replacement mineral in the groundmass. Epidote further occurs within a 2-mm-wide vein as clusters of prismatic crystals intergrown with chlorite or prehnite and is overprinted by calcite.

Pyrite, iron oxyhydroxides, and hematite

Pyrite is by far the most common sulfide mineral; it occurs in almost every rock, except for weakly altered rocks and strongly weathered near-surface rocks where pyrite has been oxidized to iron oxyhydroxides. Pyrite appears as minute anhedral to euhedral cubic grains disseminated throughout the groundmass and as a trace replacement mineral of augite and hypersthene phenocrysts together with chlorite with or without quartz.

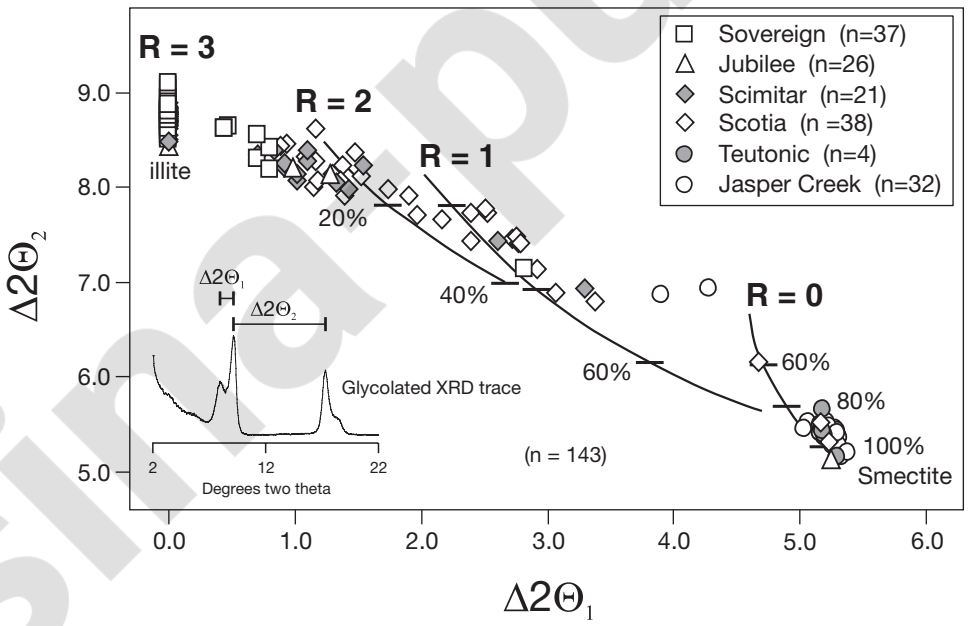

FIG. 6. A plot of $\Delta 2\Theta_1$ versus $\Delta 2\Theta_2$ showing (degree of) Reichweite (R) ordering and the proportion of smectite in interstratified illite-smectite (Watanabe, 1981; Inoue and Utada, 1983).

FIG. 7. Cross sections showing distribution of A) chlorite, interlayered chlorite-smectite, corrensite, and epidote, and B) replacement calcite. Epidote was detected only in thin section and may be more widespread than shown.

The most common occurrence of iron oxides is as orange to yellow iron oxyhydroxides that occur near surface and also at depth along fracture zones; these are interpreted to form from weathering. In contrast, hematite that occurs independently of iron oxyhydroxides is patchily distributed in drill core from the eastern margin of Scotia, Teutonic, and Jasper Creek. The strongest development of hematite is seen over a 60-m interval in the deepest drill hole at Jasper Creek—between 233 to 293 m downhole. Hematite occurs as submicroscopic disseminated grains throughout the groundmass that colors the host rock red to pale pink or purple. Where this hematite occurs as a pervasive and widespread mineral, it may have formed during cooling and degassing of the lava at subsolidus temperatures. However, hematite also occurs in quartz-hematite-pyrite and quartz-hematite veins that are cut by later calcite veins and this hematite is inferred to be hydrothermal in origin, as described below.

Calcite

Replacement calcite is a widespread alteration mineral that is most abundant at Scotia, Scimitar, and Jasper Creek, where it occurs in more than 60 percent of samples. It is less common and sporadically distributed at Jubilee, Sovereign, and Teutonic (Fig. 7B). Calcite makes up as much as 15 vol percent of the host rock; it replaces plagioclase, augite, and hypersthene phenocrysts, and locally floods the groundmass (Fig. 5F). Calcite also overprints hydrothermal adularia, albite, illite, and interstratified illite-smectite (Fig. 5C, F). At Scotia, replacement calcite is overprinted by rare smectite. Calcite also forms veins with a distribution identical to replacement calcite.

Kaolinite

Trace amounts of kaolinite were identified in XRD and SWIR (shortwave near-infrared mineral spectroscopy using the TerraSpec) profiles of near-surface iron oxyhydroxide stained samples from both Sovereign and Jubilee. This near-surface occurrence of kaolinite and the association with iron oxyhydroxides suggest that this mineral is most likely supergene.

Vein Types and Mineralogy

The Jubilee vein is the largest vein in the area, and was mined to a depth of 215 m. It is ~1,000 m in strike length and strongly lenticular, ranging from several centimeters up to 9.8 m in width, with an average width of 2.4 m. Most other veins are narrow and seldom exceed 15 cm in width but show considerable diversity in vein mineralogy (Figs. 8–10). The more common veins are described below and limited to those intercepted in drill holes that selectively targeted areas adjacent to historical workings. Details on historically mined veins are based on published descriptions (Bell and Frazer, 1912) because most old mine workings are inaccessible.

Pyrite

Thin pyrite veins with subordinate quartz were the first to form and mainly occur at Sovereign and Jubilee. They are in general less than 2 mm wide and exhibit both planar and irregular geometries. Pyrite and quartz also form the matrix cement of crackle and possible hydrothermal breccias at Sovereign. Both pyrite-quartz veins and breccia cement are cut by massive to coarsely crystalline and comb quartz veins.

Quartz

Quartz veins are the most abundant by volume, and were mined at Jubilee, Sovereign, and locally at Scotia. Quartz veins intercepted in drill core (Fig. 10) are less than 15 cm wide and predominantly composed of colorless to milky white medium- to coarse-grained massive and crystalline quartz with comb quartz commonly rimming cavities (Fig. 8A).

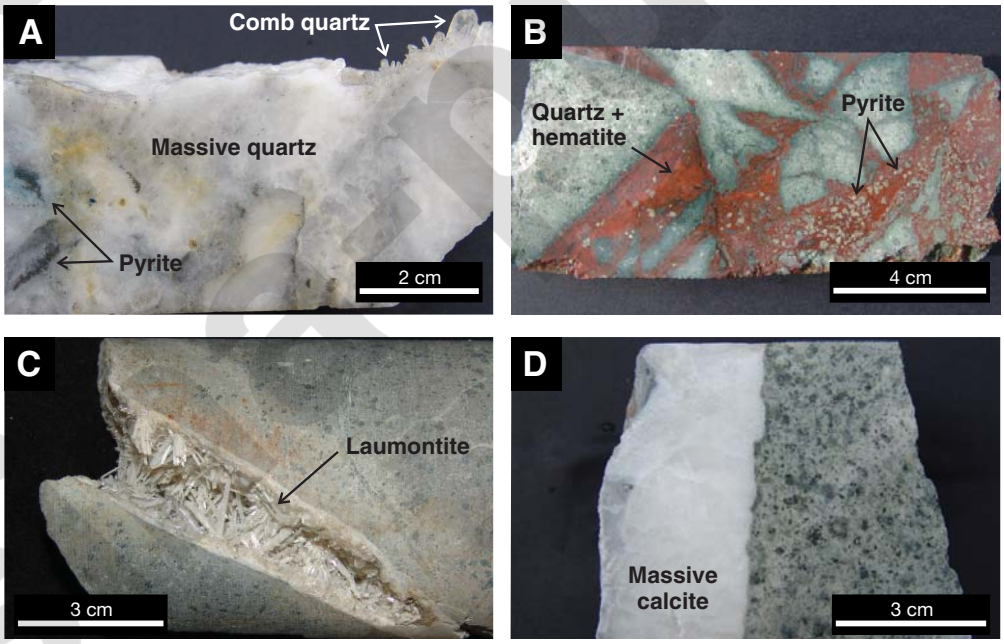

FIG. 8. Images of A) typical coarsely crystalline massive to comb quartz vein (Sovereign: ML12 140.6 m), B) cryptocrystalline quartz plus hematite vein/breccia with disseminated pyrite (Scotia: SC27 249.8 m), C) vein of acicular laumontite (Scotia: WV011 225.7 m), and D) massive calcite vein (Scotia: WV004 262.2 m).

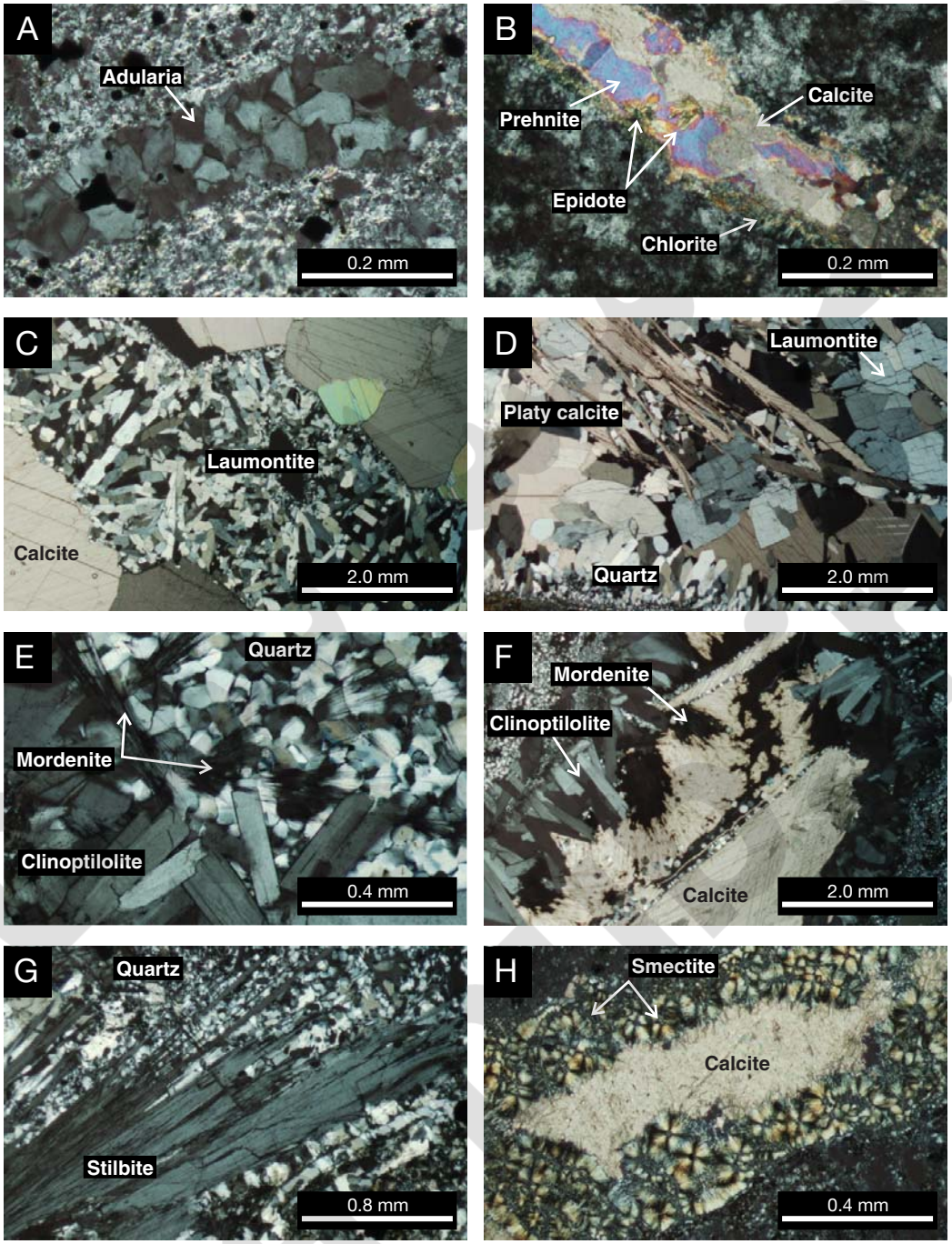

FIG. 9. Images of veins in thin section. A) Thin vein of rhombohedral adularia (Sovereign: ML12 138.9 m). B) Prehnite-epidote vein with selvages of chlorite and filled by late calcite (Sovereign: WV001 351.7 m). C) Laumontite-calcite vein with laumontite overgrowing massive calcite that exhibits weak dissolution of grain margins (Scotia: SC33 213.8 m). D) Quartz-calcite-laumontite vein with quartz selvage overgrown by platy calcite and later laumontite. Remaining open spaces are filled by later, more massive calcite (Scotia: SC27 173.8 m). E) Clinoptilolite-mordenite-quartz vein with tabular clinoptilolite overgrown by fine-grained interlocking quartz with sprays of acicular mordenite (Jasper Creek: WV009 361.8 m). F) Clinoptilolite-calcite-mordenite vein. Tabular clinoptilolite is overgrown by platy calcite that is coated by quartz. Remaining open spaces are filled by late massive calcite that encloses mordenite (Jasper Creek: WV009 380.7 m). G) Stilbite-quartz vein (Teutonic: WV010 383.0 m), and H) thin vein with botryoidal smectite and internal calcite fill (Jasper Creek: JC17 49.8 m).

Banding is weakly developed, localized, and characterized by finer-grained quartz. Casts of quartz after platy calcite are rare at Sovereign. Most veins are almost entirely quartz, although some contain minor amounts of pyrite (<1 vol %) and comb cavities are rarely filled by calcite. Rare veins contain trace to minor adularia, and adularia also forms rare monomineralic veins that are less than 1 cm wide (Fig. 9A). Base metal sulfides including sphalerite, galena, and chalcopyrite (up to

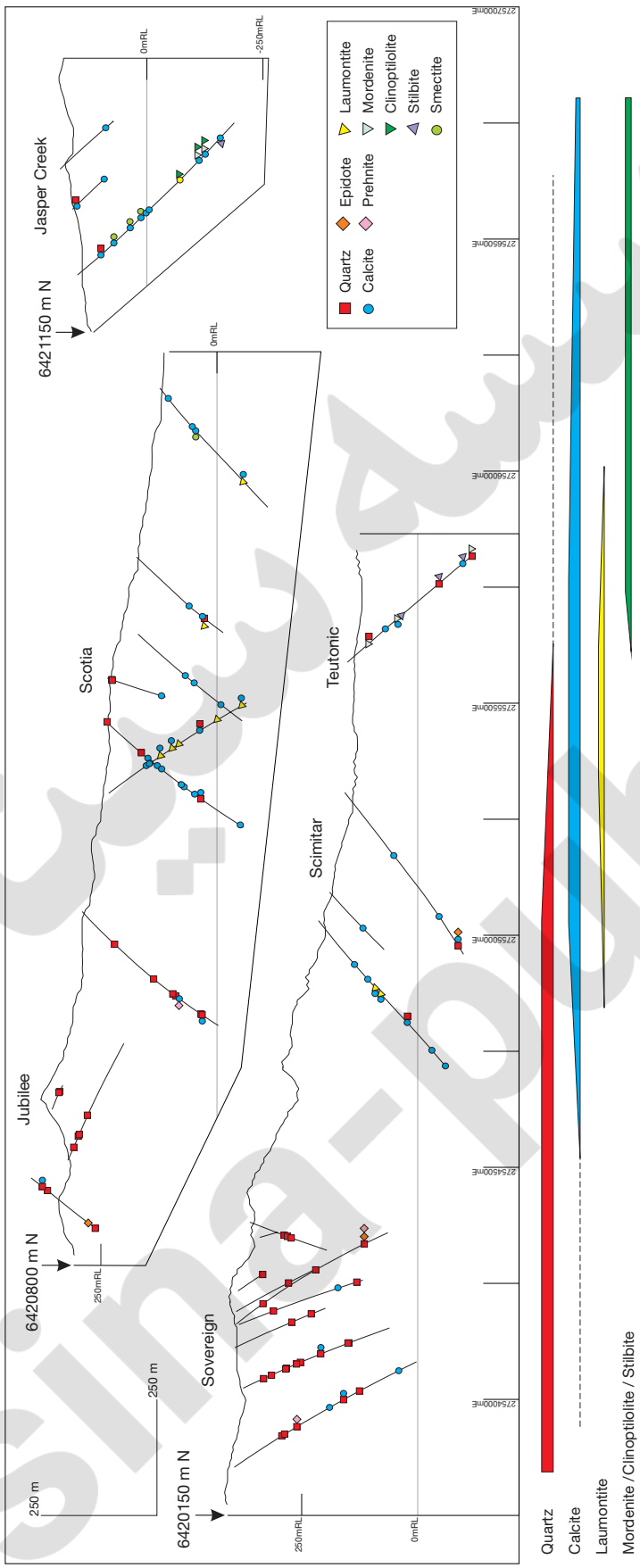

FIG. 10. Cross sections showing the distribution of vein minerals: quartz, calcite, epidote, prehnite, laumontite, mordenite, clinoptilolite, stilbite, and smectite.

3 wt % combined Zn, Pb, and Cu) and associated Ag (up to 318 g/t) were reported at depth in the Jubilee vein (Bell and Fraser, 1912; Hartley and McConnochie, 1991). Chalcopyrite, sphalerite, and galena also occur in a vein breccia at Sovereign.

Quartz-hematite-pyrite and hematite

Veins and brecciated veins of quartz-hematite-pyrite are rare and restricted to a single drill hole at Scotia. They are as much as 5 cm wide and composed of reddish-brown cryptocrystalline quartz that contains abundant micro-inclusions of disseminated hematite and irregularly distributed cubic crystals and clusters of pyrite (Fig. 8B). Adjacent host rocks are strongly altered to chlorite. Locally, these veins appear to be cut by irregular domains of cryptocrystalline quartz that lacks both hematite and pyrite. Thin, 1- to 10-mm-wide, quartz-hematite-rich veins and hematite-filled fractures that lack pyrite occur on the eastern margin of Scotia, and at Scimitar, Jasper Creek, and Teutonic. Later calcite commonly cuts or centrally fills these veins.

Zeolites (laumontite, clinoptilolite, mordenite, and stilbite)

Scotia and Scimitar contain laumontite veins, whereas Jasper Creek and Teutonic contain clinoptilolite plus mordenite or stilbite veins (Fig. 10). Laumontite veins at Scotia are up to 2 cm wide and mainly consist of microcrystalline masses or elongated prismatic crystals up to 15 mm in length (Fig. 8C). Most laumontite veins contain massive (Fig. 9C) or platy calcite (Fig. 9D), and selvages of comb quartz with or without chlorite are rare; monomineralic laumontite veins are rare. The relative timing of calcite and laumontite varies; in most veins laumontite has overgrown calcite but in some, calcite has overgrown laumontite. In the case of the former, the edges of some calcite crystals have thin reaction rims where overgrown by laumontite, indicating disequilibrium and mutually exclusive precipitation (Fig. 9C). However, no dissolution occurs where laumontite is overgrown by calcite.

At Jasper Creek and Teutonic, the main zeolite minerals are clinoptilolite, mordenite, and stilbite, which form veins that are less than 1.5 cm wide. At Jasper Creek, these veins have selvages of tabular clinoptilolite overgrown by acicular mordenite plus quartz (Fig. 9E); platy calcite and late massive calcite fill remaining open spaces (Fig. 9F). Stilbite occurs as monomineralic veins, with prismatic crystal plates, but also as quartz-stilbite veins (Fig. 9G).

Calcite

The distribution of calcite veins is broadly converse to that of quartz veins; calcite veins are mostly restricted to Scotia, Scimitar, Teutonic, and Jasper Creek (Fig. 10). Calcite most prominently occurs at Scotia as a stockwork of 1- to 15-cm-wide, massive to coarsely crystalline monomineralic veins (Fig. 8D). Elsewhere, calcite veins are typically less than 2 cm wide. Rare, weakly banded fine-grained calcite veins occur at Jasper Creek and on the eastern margin of Scotia. Massive and platy calcite further occurs in small amounts in zeolite veins where it precedes and postdates zeolite deposition. Platy calcite forms blades up to 4 cm in length that are cut by laumontite at Scotia (Fig. 9D) and are overgrown by clinoptilolite and mordenite at Jasper Creek (Fig. 9F). Quartz replacement of platy calcite is rare; it occurs as localized domains in quartz veins at Sovereign. The platy morphology indicates formation under boiling conditions (Simmons and Christenson, 1994). Calcite also occurs in the center of rare smectite veins (Fig. 9H). Due to spatial separation of quartz and calcite veins, there are few crosscutting relationships, but calcite has overgrown comb quartz in rare veins.

Paragenetic sequence of alteration and vein minerals

Figure 11 shows the generalized paragenetic sequence of alteration and vein minerals based on depositional sequence, crosscutting relationships, and the successive replacement and overprinting of alteration and vein minerals.

Thin pyrite-quartz veins were the first to form, followed by massive to weakly banded quartz veins that locally contain minor electrum and base metal sulfide minerals. Thin quartz plus adularia veins and rare monomineralic adularia veins were also deposited at this time, as were peripheral quartz-hematite ± pyrite veins. The timing of zeolite vein formation remains somewhat uncertain, but these veins appear to overlap and postdate quartz veins because quartz overgrows clinoptilolite and stilbite at Jasper Creek and Teutonic, but

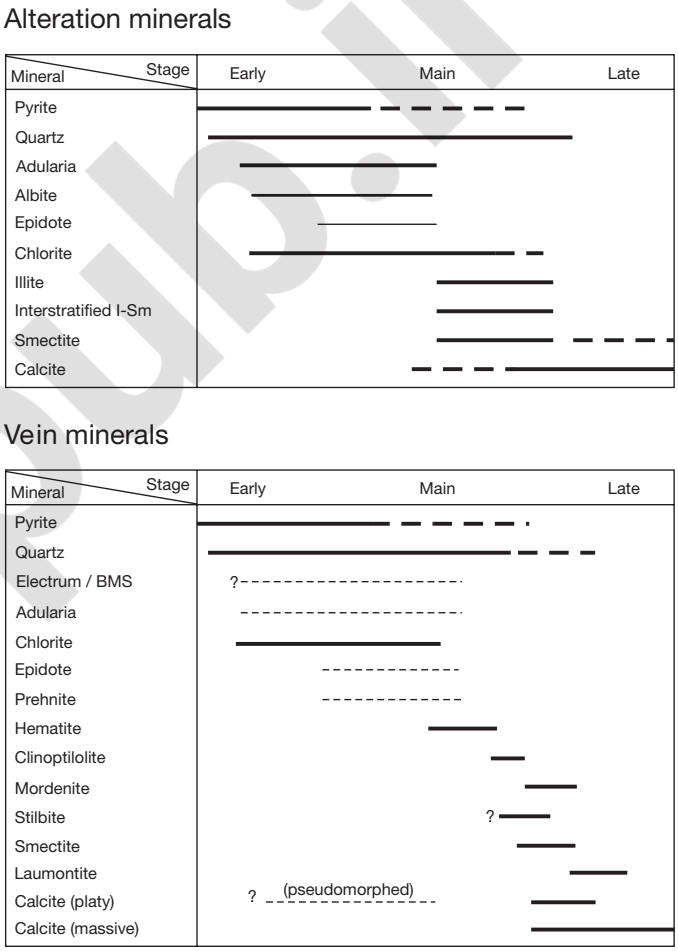

FIG. 11. Paragenetic sequence of alteration and vein minerals. Dashed lines indicate the approximate timing of mineral formation with some uncertainty. Thinner lines represent volumetrically minor minerals. BMS = base metal sulfides.

precedes laumontite at Scotia. Similarly, zeolite and calcite deposition overlap, because platy and massive calcite precede and overprint laumontite at Scotia. Calcite was the last vein mineral to form at Jasper Creek because clinoptilolite and mordenite are overprinted by later platy and massive calcite.

Host-rock alteration involved the coeval formation of quartz, adularia, albite, chlorite, rare epidote, and pyrite, which presumably was contemporaneous with the formation of quartz veins. Both adularia and albite were subsequently and variably altered to either illite, interstratified illite-smectite, or smectite. Furthermore, adularia and illite or interstratified illite-smectite are overprinted by late calcite that likely formed coevally with some calcite veins. Weathering formed supergene iron oxyhydroxides, halloysite, and kaolinite at shallow levels.

Fluid Inclusions

Fluid inclusion microthermometric measurements were made on inclusions in quartz and calcite sampled over a 500-m vertical interval. Owing to the zonation of quartz and calcite veins, quartz was the main host mineral of the fluid inclusions examined at Sovereign and Jubilee, whereas calcite was the main host mineral at Scotia, Scimitar, Teutonic, and Jasper Creek. Two types of two-phase (liquid plus vapor) fluid inclusions were observed at room temperature: abundant liquid-rich inclusions that contain 75 to 90 percent liquid and 10 to 25 vol percent vapor, and rare vapor-rich inclusions that typically contain more than 98 vol percent vapor (Fig. 12A, B). In several veins, liquid-rich and vapor-rich inclusions coexist and were likely trapped under boiling conditions (Fig. 12B; Roedder, 1984; Bodnar et al., 1985). Fluid inclusions are 3 to 35 μm in size; the cavities that host the inclusions typically have relatively straight-sided outlines, although some inclusions in quartz fill cavities have negative crystal outlines. Some calcite samples contain rare inclusions with cavities that follow a basal pinacoidal shape. Most fluid inclusions are secondary and occur along healed fractures (Fig. 12C, D). Possible primary inclusions are rare; these occur either as large isolated inclusions not associated with any obvious fractures (Fig. 12A), or as concentrated clusters of inclusions restricted to the base of some quartz crystals (Table 2). These are suspected to be primary even though we cannot demonstrate that they occur in growth zones (Roedder, 1984). Pseudosecondary fluid inclusions are similarly rare; they were documented in only two quartz samples (Fig. 12B; Sovereign: ML12 257.8 m and Jubilee: WV006 220.4 m).

Microthermometric measurements were made only on liquid-rich inclusions that homogenized by disappearance of the vapor bubble. No vapor-rich inclusions were measured because most contained very little liquid (cf. Sterner, 1992). Homogenization temperatures were determined for 755 inclusions with the temperature of final ice melting measured for 329 of these same inclusions (Table 2). Fluid inclusion measurements were made on groups of inclusions that appeared to have been trapped simultaneously. Several fluid inclusion assemblages (FIAs) were measured for some samples, and these are differentiated in Table 2. The relative timing of different FIAs could not be established, because they typically consist of spatially separated secondary inclusions in different areas of a crystal or in separate crystals. Care was taken to avoid the measurement of inclusions that were obviously necked; however, the wide T_h ranges for some FIAs that are

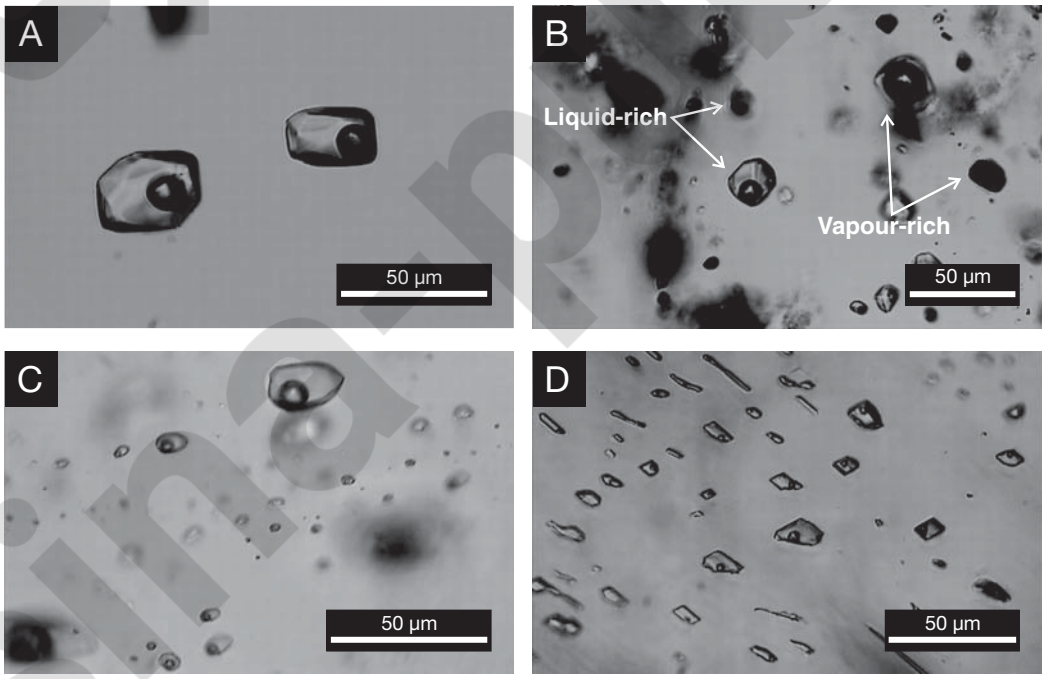

FIG. 12. Images of fluid inclusions A) isolated, possible primary liquid-rich inclusions in cavities with negative crystal outlines in quartz (Scotia: WV004 273.3 m), B) coexisting pseudosecondary, liquid-rich and vapor-rich inclusions in quartz (Jubilee: WV006 220.4 m), C) secondary liquid-rich inclusions in quartz (Sovereign: ML12 189.7 m), and D) secondary liquid-rich inclusions in calcite (Jasper Creek: JC15 135.0 m).

TABLE 2. Fluid Inclusion Heating and Freezing Results for the Waitekauri Deposits and Prospects

Sample code	Mineral	Type	T_h range (°C)	n	Avg	Mode	T_m range (°C)	n	Avg	Wt % NaCl equiv[1]	Comments
Sovereign											
ML1 83.2	Quartz	S	218–234	(13)	227	228	–0.3 to –0.8	(8)	–0.6	0.5–1.4	
ML11 286.8	Quartz	S	234–258	(6)	253	258	–0.2 to –0.6	(4)	–0.5	0.4–1.1	FIA_1 Isolated FI
	Quartz	S	228–246	(5)	238	–	0.0 to –0.1	(4)	–0.1	0.0–0.2	FIA_2 Crystal core
	Quartz	S	197–222	(7)	213	221	–0.1	(2)	–0.1	0.2	FIA_3 Crystal center
ML12 140.6	Quartz	S	225–252	(22)	232	230	0.0	(9)	0.0	0.0	Neg
ML12 189.7	Quartz	S	244–257	(18)	250	256	0.0	(9)	0.0	0.0	Rare L+V, Many Neg
	Calcite	S	245–256	(13)	253	254	0.0 to –0.4	(6)	–0.2	0.0–0.7	
ML12 257.8	Quartz	PS	236–248	(17)	242	242	–0.3 to –0.7	(8)	–0.6	0.5–1.2	Many Neg
ML13 132.0	Quartz	S	196–227	(11)	209	214	–0.2 to –0.8	(7)	–0.4	0.4–1.4	
ML13 330.8	Quartz	S	227–265	(16)	252	259	–0.4 to –0.6	(8)	–0.5	0.7–1.1	Many neg, Rare V-only
WV001 77.2	Quartz	P?	226–256	(17)	238	232	–0.5 to –0.8	(9)	–0.6	0.9–1.4	Growth zone
WV003 210.6	Quartz	P?	226–246	(10)	239	246	–0.3 to –0.6	(5)	–0.4	0.5–1.1	FIA_1 Base FI
	Quartz	P?	234–241	(7)	238	238	0.0	(6)	0.0	0.0	FIA_2 Base FI, Rare L+V
WV003 408.6	Quartz	P?	252–271	(18)	262	258	0.0 to –0.2	(9)	–0.1	0.0–0.4	Base FI, unknown acicular phase in quartz
Jubilee											
ML18 170.8	Quartz	S	236–260	(17)	250	254	–0.2 to –1.5	(8)	–1.3	0.4–2.6	
JB2 39.6	Quartz	S	208–260	(7)	232	240	–0.4 to –0.6	(2)	–0.5	0.7–1.1	Wide Th necked?
JB3 44.0	Quartz	S	218–264	(19)	239	223	–0.3 to –1.0	(9)	–0.6	0.5–1.7	Possible some necked
WV007 41.2	Calcite	S	238–261	(13)	241	240	–0.1 to –0.4	(7)	–0.3	0.2–0.7	
WV008 34.5	Quartz	S	168–239	(17)	211	196	0.0 to –0.3	(8)	–0.1	0.0–0.5	
WV008 65.5	Quartz	S	230–271	(17)	247	246	–0.2 to –0.5	(6)	–0.4	0.4–0.9	
WV006 106.2	Quartz	S	270–272	(5)	271	270	0.0 to –0.1	(4)	–0.1	0.0–0.2	FIA_1
		S	230–252	(6)	240	240	–0.4 to –0.5	(3)	–0.4	0.7–0.9	FIA_2
		S	235–255	(11)	248	253	0.0 to –0.2	(4)	–0.2	0.0–0.4	FIA_3
WV006 220.4	Quartz	PS? / S	210–243	(18)	227	225	0.0 to –0.3	(9)	–0.1	0.0–0.5	L+V, Neg
WV006 350.05	Quartz	S	239–256	(20)	245	245	–0.1 to –0.3	(8)	–0.2	0.2–0.5	
Scotia											
SC27 104.5	Calcite	S	224–247	(23)	227	226	ND				
SC27 247.6	Calcite	S	160–188	(7)	177	188	0.0	(6)	0.0	0.0	
SC28 145.0	Calcite	S	191–214	(19)	203	203	0.0	(6)	0.0	0.0	
SC28 170.4	Calcite	S	181–185	(9)	182	181	–0.2 to –0.5	(5)	–0.4	0.4–0.9	FIA_1
	Calcite	S	163–181	(6)	175	–	ND				FIA_2
SC33 167.2	Calcite	S	146–171	(14)	160	168	0.0 to –0.2	(7)	–0.1	0.0–0.4	
SC33 208.7	Quartz	S	172–196	(11)	182	181	–0.4 to –0.7	(8)	–0.5	0.7–1.2	Some neg
WV004 132.6	Calcite	S	210–224	(8)	219	220	–0.1 to –0.4	(5)	–0.2	0.2–0.7	FIA_1
		S	185–189	(5)	186	186	–0.5	(1)	–0.5	0.9	FIA_2
		S	199–227	(6)	208	–	–0.1 to –0.2	(2)	–0.2	0.2–0.4	FIA_3
WV004 158.8	Calcite	P?	203–225	(5)	209	204	–0.2 to –0.4	(4)	–0.3	0.4–0.7	FIA_1 large isolated FI
		S	184–217	(7)	202	197	ND				FIA_2
WV004 226.0	Calcite	S	212–242	(18)	227	212	0.0	(7)	0.0	0.0	
WV004 273.3	Quartz	S	216–246	(8)	228	–	0.0 to –0.5	(6)	–0.2	0.0–0.9	FIA_1
		S	225–230	(12)	227	228	–0.3 to –0.6	(3)	–0.4	0.5–1.1	FIA_2
Scimitar											
WV011 144.25	Calcite	S	208–233	(21)	221	216	–0.1	(3)	–0.1	0.2	
WV011 340.3	Quartz	S	238–310	(17)	269	256	–0.2 to –0.9	(5)	–0.5	0.4–1.6	Wide Th, necked?
	Calcite	S	253–279	(16)	263	265	0.0 to –1.1	(9)	–0.3	0.0–1.9	
WV011 481.5	Calcite	S	267–272	(11)	269	268	–0.6 to –1.0	(6)	–0.7	1.1–1.7	FIA_1
		S	250–266	(10)	259	254	–0.8 to –1.5	(4)	–1.2	1.4–2.6	FIA_2
WV012 119.6	Calcite	S	189–200	(17)	196	198	–0.3 to –0.4	(8)	–0.3	0.5–0.7	
WV015 206.2	Calcite	S	190–213	(11)	194	192	–0.2 to –0.3	(7)	–0.3	0.4–0.7	FIA_1 Pinacoidal, L+V
		S	195–227	(11)	203	200	–0.2 to –0.3	(3)	–0.2	0.4–0.7	FIA_2
WV015 406.0	Calcite	S	251–254	(14)	252	253	–0.1 to –0.2	(6)	–0.1	0.2–0.4	FIA_1
		S	248–251	(8)	249	249	–0.2 to –0.3	(4)	–0.3	0.4–0.7	FIA_2
39279	Quartz	S	235–247	(27)	226	218	–0.2 to –0.6	(10)	–0.4	0.4–1.1	
Jasper Creek											
JC15 135.0	Calcite	S	141–171	(16)	158	160	0.0 to –0.2	(7)	–0.1	0.0–0.4	
JC18 93.3	Calcite	S	157–204	(5)	174	–	ND				Plate disintegrated
JC19 67.9	Calcite	S	179–185	(10)	182	184	–0.1	(2)	–0.1	0.2	Mordenite in calcite
WV009 64.8	Calcite	S	155–201	(14)	179	182	0.0 to –0.2	(8)	–0.1	0.0–0.4	
WV009 198.2	Calcite	S	132–152	(22)	143	142	ND				Pinacoidal, No ice seen
Teutonic											
WV010 126.4	Calcite	S	166–173	(16)	168	167	0.0 to –0.3	(8)	–0.2	0.0–0.5	

Notes: Base FI = cluster of fluid inclusions restricted to crystal base and possibly of primary origin, Iso FI = isolated fluid inclusions of possible primary origin, L+V = coexisting two-phase liquid-rich and vapor-rich inclusions, ND = no data due to either no ice seen on freezing or as in the case of sample JC18 93.3 m the plate disintegrated, FIA = fluid inclusion assemblage (number defines group but not sequence of formation), Neg = inclusions fill negative crystal shaped cavities, P = primary fluid inclusions, PS = pseudosecondary fluid inclusions, S = secondary fluid inclusions, T_h = homogenization temperature, T_m = ice melting temperature

[1]Wt % NaCl equiv calculated from Bodnar (1993)

skewed by one or two inconsistent values suggest the inadvertent measurement of necked fluid inclusions (Table 2).

Homogenization temperatures (T_h) for primary, pseudosecondary, and secondary inclusions hosted in quartz from Sovereign and Jubilee overlap, ranging from 168° to 272°C (Fig. 13). Secondary inclusions in calcite and those in rare quartz from Scimitar have a T_h range of 189° to 310°C. At Scotia, secondary inclusions predominately hosted in calcite have a T_h range of 146° to 247°C, whereas those from Jasper Creek that are exclusively hosted in calcite have lower T_h values that range from 132° to 204°C. Secondary inclusions in a single calcite sample from Teutonic have T_h values between 166° and 173°C (Fig. 13).

In Figure 14, the average T_h values for inclusions in quartz and calcite are plotted as a function of sample location. Even though most inclusions are secondary, the average T_h values generally increase with depth, with the deepest samples from Scimitar recording the highest values. Overall, the average T_h values are lesser to the east, although there are exceptions, where some samples have lower average T_h values compared to surrounding samples. We interpret these lower T_h values as secondary fluid inclusions that have trapped cooler fluids at a later stage. At Jasper Creek, greater T_h values at shallow levels contrast with a single sample at greater depth that has lower T_h value; this could reflect a temperature inversion, but more data are required to substantiate this hypothesis.

Final ice melting temperatures (T_m) for quartz and calcite range from 0.0° to –1.5°C (Fig. 13B), and correspond to apparent salinities of up to 2.6 wt percent NaCl equiv (Bodnar, 1993). Many inclusions in calcite have T_m values of 0.0°C and have trapped dilute fluids.

Stable Isotopes

Table 3 presents $\delta^{18}O$ and $\delta^{13}C$ values of quartz and calcite from veins in the Waitekauri area. Owing to the overall mineral zonation in the area, quartz vein samples are most abundant in the western deposits, whereas calcite vein samples are most abundant in the eastern prospects.

Quartz has $\delta^{18}O$ values that range from 4.1 to 9.7 per mil, with an overall average value of 6.7 per mil (Table 3, Fig. 15). Calcite has $\delta^{18}O$ values that range from 1.7 to 18.6 per mil, with an average value of 6.9 per mil, but if the obvious outlier at 18.6 per mil is excluded, then the average value decreases to 6.1 per mil (Table 3). The $\delta^{13}C$ values of calcite range from –11.7 to –5.9 per mil, and if we exclude the outlier at –11.7 per mil, the average value is –7.0 per mil (Table 3).

Stable isotope samples came from veins that have corresponding fluid inclusion data. Applying published mineral-water fractionation factors for quartz (Matsuhisa et al., 1979) and calcite (Friedman and O'Neil, 1977), we used the modal homogenization temperatures of each sample as a proxy for trapping temperatures to calculate the isotopic composition of the fluid that formed the veins. Many of the calculated $\delta^{18}O_{water}$ values are close to the –5 per mil value that is commonly ascribed to meteoric water at the nearby Golden Cross deposit (de Ronde and Blattner, 1988; Simpson et al., 1995; Simmons et al., 2000), but there is considerable scatter around this value for both quartz and calcite (Table 3). The observed scatter in calculated $\delta^{18}O_{water}$ values may reflect several factors, including (1) analytical errors in measuring fluid inclusion homogenization temperatures and/or stable isotope values of quartz and calcite, (2) lack of precision in fluid inclusion or isotopic data, (3) sample heterogeneity, (4) water-rock interaction, (5) addition of fluids other than meteoric water, or (6) some combination of the above.

Our data do not allow us to rigorously test some of the above possibilities, but uncertainties in the temperature of mineral formation could account for much of the variability in calculated $\delta^{18}O_{water}$ values. In Figure 15, error bars for the temperature and $\delta^{18}O_{mineral}$ values have been added. The stable isotope data have reproducibilities better than ± 0.1 per mil, which is less than the width of the symbols on the diagram. Many of the fluid inclusion T_h values for individual samples show a range of results that vary ±10°C around the average value (Table 2), so we have used ±10°C as the error bars for the T_h values.

Figure 15A shows that most calculated $\delta^{18}O_{water}$ values, or their error bars, lie within the –4 to –6 per mil range that is close to the accepted –5 per mil value for meteoric water in the area at the time (de Ronde and Blattner, 1988; Simpson et al., 1995; Simmons et al., 2000). Three quartz samples have calculated $\delta^{18}O_{water}$ values that plot below this range, and three quartz samples have calculated $\delta^{18}O_{water}$ values that plot above this range. Although various geologic processes could be invoked to explain this scatter, the simplest interpretation is that the relatively symmetric scatter to more enriched and depleted calculated $\delta^{18}O_{water}$ values reflects scatter due to use of T_h values from secondary inclusions in quartz (Fig. 15A).

Figure 15B shows that, including error bars, most calculated $\delta^{18}O_{water}$ values derived from calcite also fall within the –6 to –4 per mil band that is consistent with formation from meteoric water with a $\delta^{18}O_{water}$ value of –5 per mil. However, in contrast to quartz, the calculated $\delta^{18}O_{water}$ values for calcite show asymmetric scatter; four samples have more enriched $\delta^{18}O_{water}$ values that lie in the 0 to –2 per mil range. The most likely geologic causes of ^{18}O enrichment of the water are (1) mixing with a fluid that is enriched in ^{18}O, such as magmatic water, andesitic water, or basinal brines, (2) water-rock interaction, and (3) steam loss from the hydrothermal fluid. Given that the calcite formed late in the hydrothermal system, it likely formed from CO_2-rich steam-heated waters that would reflect the isotopic composition of local meteoric water (Simmons et al., 2000), so possibilities (1) and (2) are unlikely. Single-step steam loss from a hydrothermal fluid can produce a shift in $\delta^{18}O$ values of approximately 2 per mil (Giggenbach, 1992), which is less than the 3 to 5 per mil shift suggested by our data. Taken together, these results suggest that expected geologic processes cannot reasonably account for the apparent enrichment of $\delta^{18}O_{water}$ values that are suggested by Figure 15B.

An alternative explanation is that the calcite did form from meteoric water, but at a temperature that differed from the homogenization temperatures of the secondary inclusions that were measured during this study. We used published calcite-water fractionation factors (Friedman and O'Neil, 1977), a $\delta^{18}O_{water}$ value of –5 per mil, and the isotopic composition of the calcite to model the temperature of the calcite-forming fluid. Calculated temperatures ranged from 111° to 181°C; these were 30° to 57°C below the minimum measured homogenization temperature for each sample, and 49° to 63°C

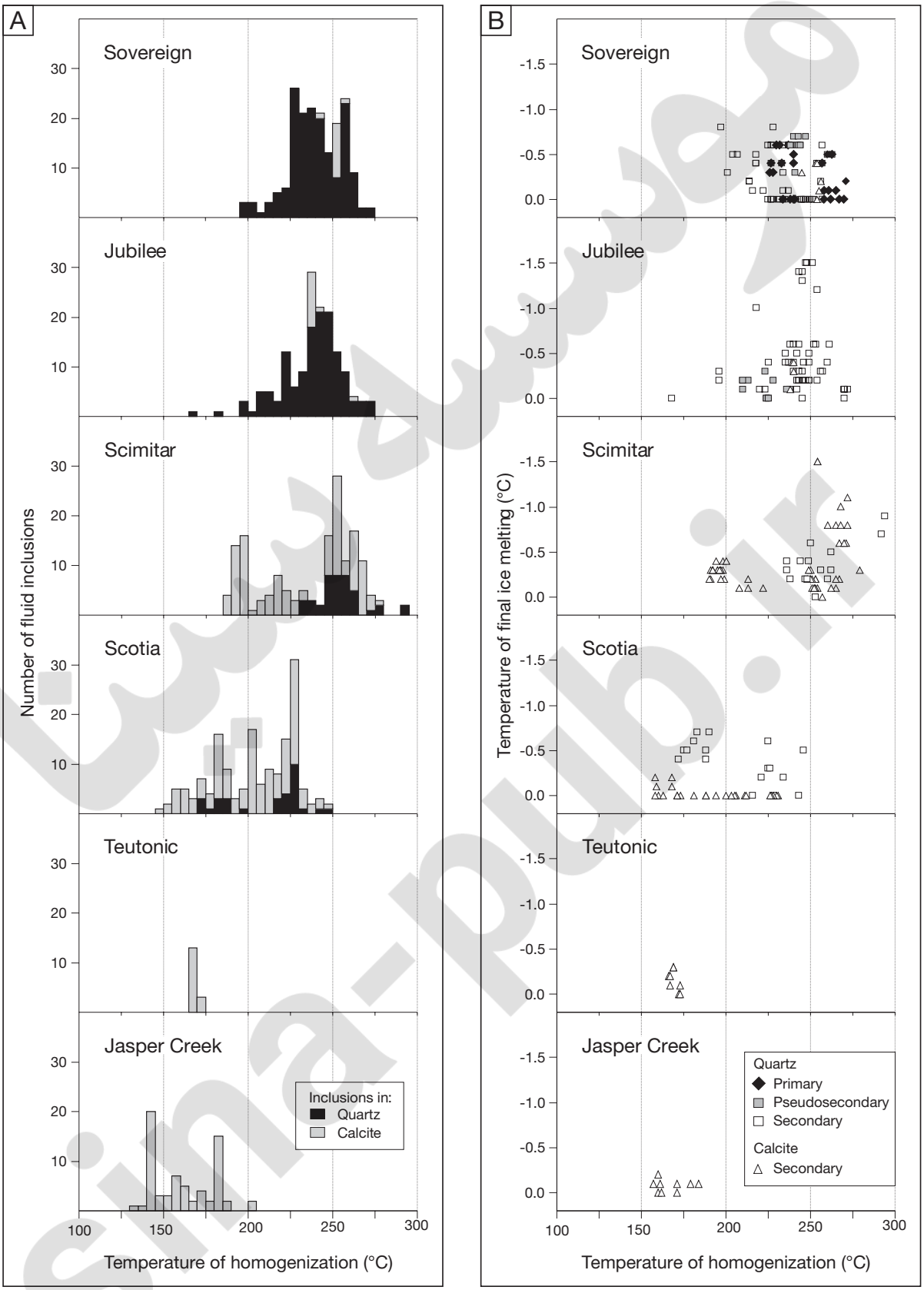

FIG. 13. Fluid inclusion microthermometry results plotted for individual deposits and prospects. A) Homogenization temperature versus frequency plots and B) homogenization temperature versus temperature of final ice melting for primary, pseudosecondary, and secondary fluid inclusions.

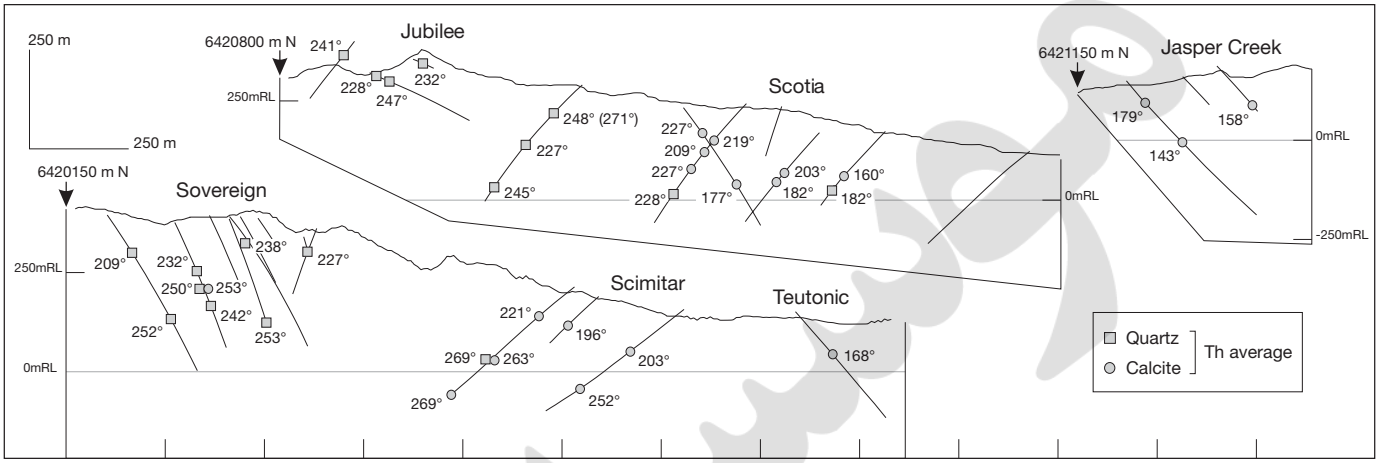

FIG. 14. Cross sections showing average T_h values for individual fluid inclusion assemblages plotted as a function of sample locations for quartz and calcite. In the case of samples with multiple fluid inclusion assemblages, the greatest average T_h value is plotted. In general, temperatures increase with depth and decrease toward the east. At Jasper Creek, greater T_h values occur at shallow levels. A single sample with lesser T_h values at depth may reflect a temperature inversion, but more data are required to test this hypothesis.

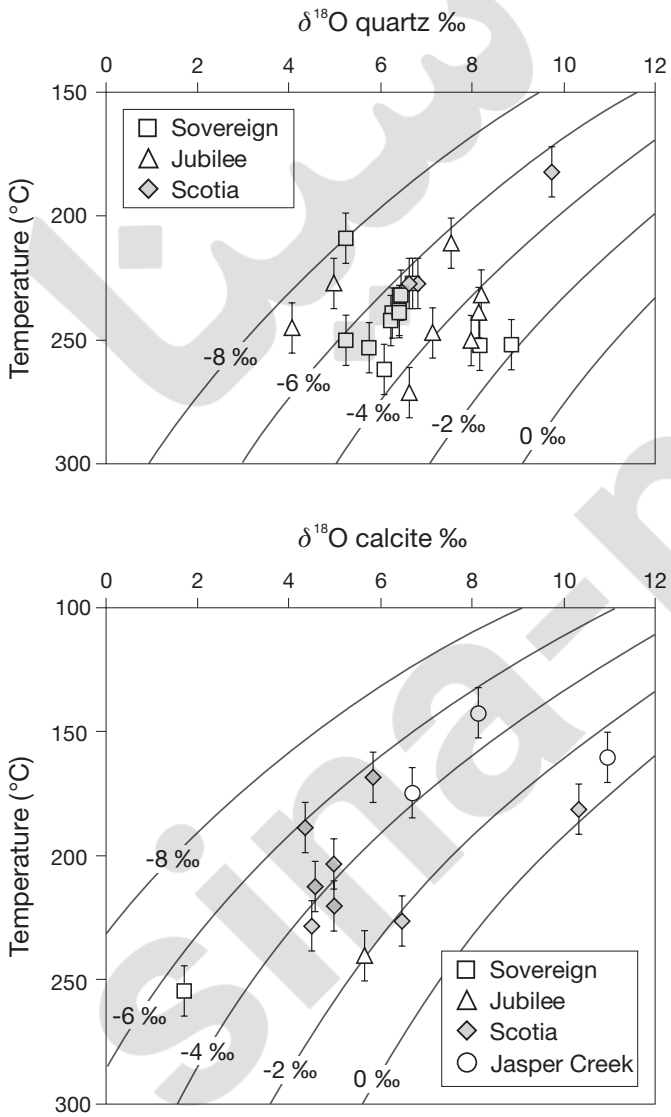

below the modal homogenization temperatures. If valid, these results suggest that at least some of the vein calcite in the Waitekauri hydrothermal system formed during a late-stage cooling event, and that either (1) the veins were occasionally subjected to pulses of higher-temperature hydrothermal fluids that trapped the measured secondary inclusions, or (2) the $\delta^{18}O$ values of calcite in the veins continued to re-equilibrate with meteoric water at lower temperatures as the system cooled. We prefer the latter explanation, as it appears to be the most reasonable, but we acknowledge that critical testing of this hypothesis would require additional work.

In summary, we conclude that quartz and calcite in veins from the Waitekauri area likely formed from meteoric water, similar to interpretations for most adularia-sericite epithermal deposits worldwide (e.g., Simmons et al., 2005, and references therein). Critical analysis of the calcite data suggests that at least some data reflect an overall cooling event during the formation of late-stage calcite veins.

Discussion

The hydrothermal processes that led to alteration and vein formation in the Waitekauri area can be interpreted in the context of modern geothermal fields, where the mineral products of alteration and deposition can be directly related to fluids of known temperature, pressure, and chemical composition (e.g., White, 1955; 1981; Henley and Ellis, 1983; Henley and Hedenquist, 1986; Reyes, 1990; Simmons and

FIG. 15. Stable isotope data for quartz and calcite. A. $\delta^{18}O$ composition of quartz vs. fluid inclusion homogenization temperatures. Isopleths show the calculated $\delta^{18}O$ values of water in equilibrium with quartz as a function of temperature, which was calculated using published mineral-water fractionation factors for quartz (Matsuhisa et al., 1979). B. $\delta^{18}O$ composition of calcite vs. fluid inclusion homogenization temperatures. Isopleths show the calculated $\delta^{18}O$ values of water in equilibrium with calcite as function of temperature, which were calculated using published mineral-water fractionation factors for calcite (Friedman and O'Neil, 1977).

TABLE 3. Oxygen and Carbon Isotope Values with Corresponding Fluid Inclusion Results and Calculated Water Compositions for the Waitekauri Deposits and Prospects

Sample code	Mineral	$\delta^{18}O$ (‰)	$\delta^{13}C$ (‰)	T_h Mode (°C)	$\delta^{18}O$ water (‰)	Comments
Sovereign						
ML1 83.2	Quartz	6.7		228	–5.5	
ML11 286.8	Quartz	5.7		258	–5.2	
ML12 140.6	Quartz	6.4		230	–5.5	
ML12 189.7	Quartz	5.2		256	–5.8	
ML12 257.8	Quartz	6.2		242	–5.2	
ML13 132.0	Quartz	5.2		214	–8.0	
ML13 330.8	Quartz	8.2		259	–2.6	
ML13 330.8	Quartz	8.8		259	–1.9	Duplicate of above
WV001 77.2	Quartz	6.4		232	–5.3	
WV003 210.6	Quartz	6.3		246	–5.4	
WV003 210.6	Quartz	6.4		246	–5.2	Duplicate of above
WV003 408.6	Quartz	6.0		258	–4.5	
Jubilee						
ML18 170.8	Quartz	8.0		254	–3.1	
JB2 39.6	Quartz	8.2		240	–3.8	
JB3 44.0	Quartz	8.1		236	–3.5	
WV008 34.5	Quartz	7.5		196	–5.6	
WV008 65.5	Quartz	7.1		246	–4.1	
WV006 106.2	Quartz	6.6		270	–3.6	
WV006 220.4	Quartz	5.0		225	–7.2	
WV006 350.05	Quartz	4.1		245	–7.2	
Scotia						
SC33 208.7	Quartz	9.7		181	–5.3	
WV004 273.3	Quartz	6.6		228	–5.6	
WV004 273.3	Quartz	6.8		228	–5.4	Duplicate of above
Sovereign						
ML12 189.7	Calcite	1.7	–8.7	254	–5.4	
Jubilee						
WV007 41.2	Calcite	5.6	–5.9	240	–2.1	
Scotia						
SC27 104.0	Calcite	6.4	–7.3	226	–1.9	
SC27 247.6	Calcite	4.3	–7.8	188	–6.6	
SC28 145.0	Calcite	5.0	–8.0	203	–4.4	
SC33 167.0	Calcite	5.8	–6.8	168	–6.1	
SC33 208.7	Calcite	10.3	–6.2	181	–0.3	
WV004 132.6	Calcite	4.9	–7.0	220	–3.7	
WV004 226.0	Calcite	4.6	–7.4	212	–3.6	
WV004 273.2	Calcite	4.5	–7.2	228	–3.7	
Jasper Creek						
JC15 135.0	Calcite	11.0	–6.7	160	–1.0	
JC18 93.3	Calcite	6.6	–6.4	174	–4.5	
JC18 93.3	Calcite	6.7	–6.4	174	–4.4	Duplicate of above
WV009 64.8	Calcite	18.6	–11.7	182	7.9	
WV009 198.0	Calcite	8.1	–6.6	142	–5.2	

Notes: T_h = homogenization temperature

Browne, 2000). Table 4 presents a summary of hydrothermal alteration, vein types, fluid inclusion data, and stable isotope data for the Waitekauri deposits and prospects.

Fluid flow and host-rock water/rock ratios

Faults and fractures served as conduits for the hydrothermal fluids that formed the Jubilee vein and veins at Sovereign and Scotia. The intense and pervasive alteration of volcanic rocks at Sovereign and Jubilee also reflects significant flow of hydrothermal fluids through the host rocks, whereas less altered rocks at Scotia, Teutonic, and Jasper Creek suggest lower water/rock ratios. In modern geothermal fields, areas of high water/rock ratios and fluid flow correlate with the occurrence of replacement adularia or coexisting hydrothermal albite plus adularia (Browne and Ellis, 1970; Browne, 1978). By contrast, hydrothermal albite without adularia occurs in areas of lower water/rock ratios (Browne, 1978). Laumontite and prehnite also indicate areas of lower water/rock ratios (Reyes, 1990). Widespread adularia at Sovereign and the adularia carapace at Scotia and Jasper Creek are interpreted to reflect areas of high water/rock ratios and inferred high permeability when adularia formed (Fig. 4). Coexisting adularia and albite also reflect areas of significant water/rock ratios at Jubilee and Scotia, although this association is uncommon. Hydrothermal albite below the adularia carapace at Scotia and laumontite veins at Scotia and Scimitar represent areas of lower

TABLE 4. Comparison of Hydrothermal Alteration, Vein Mineralogy, Fluid Inclusion, and Stable Isotope Data for the Sovereign, Jubilee, Scimitar, Scotia, Teutonic, and Jasper Creek Deposits and Prospects

	Sovereign	Jubilee	Scimitar	Scotia	Teutonic	Jasper Creek
Production Au-Ag bullion	229 kg	140 kg	–	23 kg	–	–
Host rock	Andesite breccia and pyroclastics, rhyolite dikes	Andesite flows and rhyolite dikes	Andesite flows	Dacite flows	Dacite flows	Andesite flows
Host-rock alteration (mineral occurrences as percentage of sample) [1]						
Quartz	100	100	100	100	100	90
Adularia	79	53	4	46	0	46
Albite	2	35	0	49	0	0
Chlorite	76	71	88	86	50	39
Epidote [2]	25	20	10	0	0	0
Illite	74	88	38	31	0	0
Illite-smectite	12	12	54	51	0	5
Smectite	0	0	0	9	100	93
Calcite	19	35	79	66	17	61
Veins						
Dominate vein type	Quartz	Quartz	Calcite	Quartz/calcite	Zeolite	Calcite/zeolite
Major veins	0.1–1 m wide	990 × 215 × 2.5 m wide Jubilee vein	–	0.1–0.4 m wide stockwork	–	–
Vein types	Quartz pyrite, rare calcite	Quartz pyrite, rare calcite	Calcite rare laumontite rare quartz	Calcite, quartz laumontite, hematite, pyrite	Mordenite, stilbite calcite, quartz, smectite	Calcite clinoptilolite, mordenite, smectite, rare quartz
Ore and sulfide minerals	Electrum, chalcopyrite, galena, sphalerite, pyrite	Electrum, chalcopyrite, galena, sphalerite, pyrite	–	Electrum argentite	–	–
Fluid inclusions						
T_h range and average	196°–271° 241° (Qtz)	168°–272° 239° (Qtz)	189°–310° 232° (Ct)	146°–247° 204° (Ct)	166°–173° 168° (Ct)	132°–204° 162° (Ct)
Salinity (wt % NaCl equiv)	0.0–1.4	0.0–2.6	0.0–2.6	0.0–1.2	0.0–0.5	0.0–0.4
Paleowater table depth [3]	690 m asl	(750 m asl)	(575 m asl)	(450 m asl)	(150 m asl)	(225 m asl)
Stable isotopes						
$\delta^{18}O$ range and mineral	5.2–8.8 (Qtz) 1.7 (Ct)	4.1–8.2 (Qtz) 5.6 (Ct)	–	6.6–9.7 (Qtz) 4.3–10.3 (Ct)	–	6.6–11.0 (Ct)
$\delta^{18}O$ H_2O calculated	–1.9 to –8.0 (Qtz) –5.4 (Ct)	–3.1 to –7.2 (Qtz) –2.1 (Ct)	–	–5.3 to –5.6 (Qtz) –0.3 to –6.6 (Ct)	–	–1.0 to –5.2 (Ct)

Abbreviations: Qtz = quartz, Ct = calcite

[1] Mineral percentages were determined by dividing the number of samples containing a given mineral, as determined by XRD and petrography, by the total number of samples studied

[2] Mineral % based on petrography only

[3] Paleowater table elevations in parentheses as measured using current elevations represent the best-fit values that account for most data points (see text)

water/rock ratios and inferred lower permeability (Browne and Ellis, 1970). Taken together, the available data indicate that water/rock ratios were greatest in the west (Sovereign and Jubilee), more variable and possibly stratified in the center (Scimitar and Scotia), and generally less to the east (Jasper Creek and Teutonic).

Temperature of alteration and vein formation

The formation temperature of hydrothermal minerals can be inferred from temperature-sensitive minerals, such as clay, zeolite, and calc-silicate minerals, and from fluid inclusion measurements. The derived temperatures represent two different time and space scales. Temperatures inferred from alteration minerals reflect conditions that prevailed during hydrothermal activity, whereas those from fluid inclusions reflect short periods of geologic time when the fluid was trapped. Because most fluid inclusions that we measured in this study are secondary, they record a temperature following formation of the host mineral and may not reflect the temperature of vein formation. Clay mineral formation can be

controlled by temperature but also by the chemistry of altering fluids, rock composition, and water/rock ratios (Essene and Peacor, 1995; Tillick et al., 2001).

In geothermal fields, the following minerals form over restricted temperature intervals (Steiner, 1968, 1977; Bird et al., 1984; Reyes, 1990; Okada et al., 2000): epidote (>240°C), prehnite (>240°C), illite (>220°C), interstratified illite-smectite (<220°–150°C), smectite (<150°C (New Zealand) to <170°C (Philippines)), laumontite (<220°–120°C), clinoptilolite (200°–110°C), and mordenite (<200°).

At Sovereign, Jubilee and the western margin of Scimitar, the occurrence of illite (Fig. 4B), local epidote (Fig. 7A), and prehnite indicate formation temperatures of at least 220° to greater than 240°; consistent with average quartz fluid inclusion T_h values of 241°C for Sovereign and 239°C for Jubilee (Fig. 14). At Scimitar and Scotia, illite grades eastward into interstratified illite-smectite with increasing amounts of smectite (Fig. 4B); together with localized laumontite veins (Fig. 10), these minerals suggest temperatures of greater than 220°C in the west and less than 220°C toward the east. These temperatures are consistent with average T_h values in quartz and calcite that generally decrease from west to east, from 269° to 196°C at Scimitar and from 228° to 160°C at Scotia (Fig. 14). Smectite and localized interstratified illite-smectite at Teutonic and Jasper Creek together with clinoptilolite and mordenite veins suggest formation temperatures of less than 200°C; these inferred temperatures overlap with calcite fluid inclusion T_h values that range from 189° to 132°C, with an average of 162°C (Fig. 14).

Overall, there is good agreement between temperatures inferred from mineral stabilities and fluid inclusion homogenization temperatures. Temperatures were greater than 240°C at Sovereign and Jubilee in the west, between ~230° and ~170°C at Scotia, and between ~170° and 140°C at Teutonic and Jasper Creek.

Fluid composition inferred from alteration minerals and fluid inclusions

The alteration mineral association of quartz, adularia, albite, chlorite, illite, interstratified illite-smectite, smectite, calcite, and pyrite in the Waitekauri area is identical to that in geothermal fields that form from near-neutral pH chloride water (Browne and Ellis, 1970; Henley and Ellis, 1983; Giggenbach, 1992; Simmons and Browne, 2000). In these geothermal fluids, chloride is the dominant anion, ranging from 0.1 to 1 wt percent Cl, and the fluids contain as much as 3 wt percent CO_2, which is coupled with tens to hundreds of ppm H_2S (Simmons et al, 2005); the latter is an important ligand for the transport of Au and Ag as bisulfide complexes (Seward and Barnes, 1997). At the Waitekauri deposits and prospects, zeolite veins coupled with replacement and vein calcite further suggest that the chloride waters contained low to intermediate concentrations of dissolved CO_2 (Fig. 16), comparable to those at the Waiotapu geothermal field, which has both these minerals and chloride waters with 0.04 to 0.22 wt percent (0.01–0.05 molal) CO_2 (Hedenquist and Browne, 1989). At Waiotapu, zeolites (mordenite, laumontite, and wairakite) and calcite are mutually exclusive in most places, except in

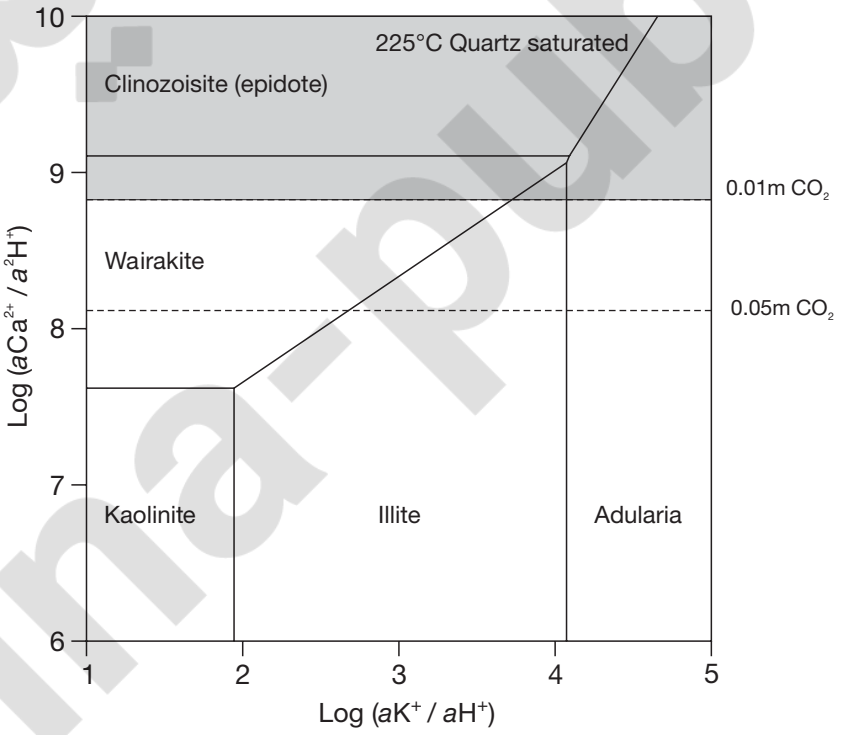

FIG. 16. Activity diagram showing the stability of calcium and potassium aluminosilicates at 225°C in equilibrium with quartz, and the calcite stability field at 0.01 and 0.05 molal CO_2 (Hedenquist and Browne, 1989). The shaded area represents the calcite stability field at 0.01 molal CO_2; under this condition calcite supersedes the formation of epidote and some wairakite.

rare cavities where they alternate in bands. In the Waitekauri area, thin zeolite veins commonly contain calcite; mordenite and clinoptilolite are both overgrown by massive and platy calcite, whereas massive or platy calcite is typically overgrown by laumontite. In the latter case, calcite has thin dissolution rims where it is overgrown by laumontite, which indicates disequilibrium and mutually exclusive deposition. This alternation may be due to fluctuating CO_2 concentrations caused by boiling. Boiling results in the deposition of platy calcite near the point of boiling (Simmons and Christenson, 1994) with partitioning of CO_2 into the steam phase resulting in chloride waters with significantly lower CO_2 content that would favor zeolite formation. Because zeolites and calcite alternate, this suggests that the boiling front fluctuated in position, resulting in variable CO_2 concentrations that at times favored zeolite formation, and at other times, calcite deposition (Fig. 16). The lack of zeolite minerals at Sovereign and Jubilee suggests that greater CO_2 concentrations here may have precluded their formation.

Thin quartz-hematite veins with or without pyrite together with hematite alteration of the host rock are locally developed on the eastern margin of Scotia, as well as at Teutonic and Jasper Creek. The presence of hematite suggests change in the redox state of the chloride waters that stabilized hematite over pyrite (Vaughan and Craig, 1997). This change could have resulted from the mixing of chloride waters with more oxygenated groundwaters.

Fluid inclusion final ice melting temperatures of –1.5°C for quartz and calcite correspond to dilute fluids with apparent salinities of up to 2.6 wt percent NaCl (Bodnar, 1993). Alternatively, these final ice melting temperatures could be explained by up to 3.5 wt percent CO_2 (Hedenquist and Henley, 1985). The presence of zeolites indicates low CO_2 concentrations in the fluids (Hedenquist and Browne, 1989), so most of the freezing point depression likely reflects dissolved salts rather than dissolved gas. Despite uncertainty with respect to the timing of secondary inclusion entrapment, the apparent salinity and/or CO_2 content for fluid inclusions appear to decrease from the west to east, possibly due to boiling and gas loss, dilution due to mixing, or a combination of the two (Fig. 13B).

Late-stage replacement calcite and overprinting smectite, possibly together with some monomineralic calcite veins, may have formed from steam-heated CO_2-rich waters. In geothermal fields, these steam-heated CO_2-rich fluids that contain greater than 1 wt percent CO_2 originate by the condensation of CO_2 into shallow groundwaters that occur above and drape the margins of the upflow zone (Hedenquist and Stewart, 1985; Simmons and Christenson, 1994). During thermal collapse, these steam-heated CO_2-rich waters can also descend into and overprint the former zone of upwelling chloride waters (Simmons et al., 2000) with heating of these fluids on descent resulting in the deposition of calcite due to its inverse solubility with respect to temperature (Ellis, 1959; Simmons and Christenson, 1994).

Depth of formation

The depth of vein formation below the paleowater table can be estimated from the trapping temperature and salinity of primary fluid inclusions that show evidence of boiling in the form of coexisting liquid- and vapor-rich inclusions (Roedder, 1984). Under hydrostatic conditions (Haas, 1971), suspected primary, liquid-rich inclusions that coexist with vapor-rich inclusions in a quartz vein at Sovereign, with an average trapping temperature (T_T) of 253°C and dilute salinity (<1 wt % NaCl equiv) indicate that the paleowater table was 690 m above sea level relative to current elevations (Fig. 17). Paleowater table elevations above Jubilee, Scimitar, Scotia, Teutonic, and Jasper Creek have been estimated from secondary inclusions in quartz and calcite and are based on several assumptions. At each of these locations the boiling point for depth curve is fitted for a single centrally located sample using the maximum T_h value (excluding obvious outliers) and assumes entrapment under boiling conditions. Although these samples did not show fluid inclusion evidence of boiling in the form of coexisting liquid-rich and vapor-rich inclusions, the occurrence of platy calcite, quartz pseudomorphs of platy calcite, vein adularia, and, indirectly, common replacement adularia (Fig. 17) indicate that the fluids were commonly boiling throughout the Waitekauri area (Browne and Ellis, 1970; Simmons and Christenson, 1994). The highest average T_h was used because this reflects the upper limit of temperature conditions and corresponds to the highest elevation of the water table. However, because these calculations are based on secondary inclusions trapped at some time following vein formation, they may not represent the temperature at which the host mineral formed and therefore the estimated paleodepths must be treated with caution. Nonetheless, the paleowater table above the Jubilee, Scimitar, Scotia, Jasper Creek, and Teutonic prospects, based on the maximum T_h of secondary inclusions and assuming boiling conditions, occurs at 750, 575, 450, 225, and 150 m above sea level (using current elevations), respectively, spanning a 600-m vertical interval and corresponding to at least 35 to 560 m erosion (Fig. 17). These calculated depths indicate that the veins in the east formed at shallower levels than the veins to the west. A shallow formation depth at Jasper Creek is consistent with the occurrence of a hydrothermal eruption breccia that presumably had a maximum focal depth of 90 m, as documented in geothermal fields (cf. Browne and Lawless, 2001). Moreover, alteration and vein minerals indicate cooler temperatures of formation to the east, suggesting shallower formation depths consistent with the fluid inclusion calculations.

Figure 18 shows the estimated paleowater table elevations from the Waitekauri area determined for a greater number of samples. Most depths were calculated based on secondary inclusions using the highest T_h values and assuming trapping under near-boiling conditions. If all inclusions were trapped at the same time from fluids in a single geothermal system, then the water table above Sovereign, Jubilee, and Jasper Creek appears to be relatively flat lying (3°–10° dip), but is steeply inclined (35°–47° dip) over Scotia and Scimitar. Although a steeply dipping water table is possible, it is more likely that the apparent steep dip is due to postmineralization offset by one or more faults with a combined vertical displacement of more than 100 m or the trapping of inclusions at different times from either a heating or cooling fluid. Alternatively, this apparent slope may represent the boundary between two separate geothermal systems that formed at different times and at different elevations.

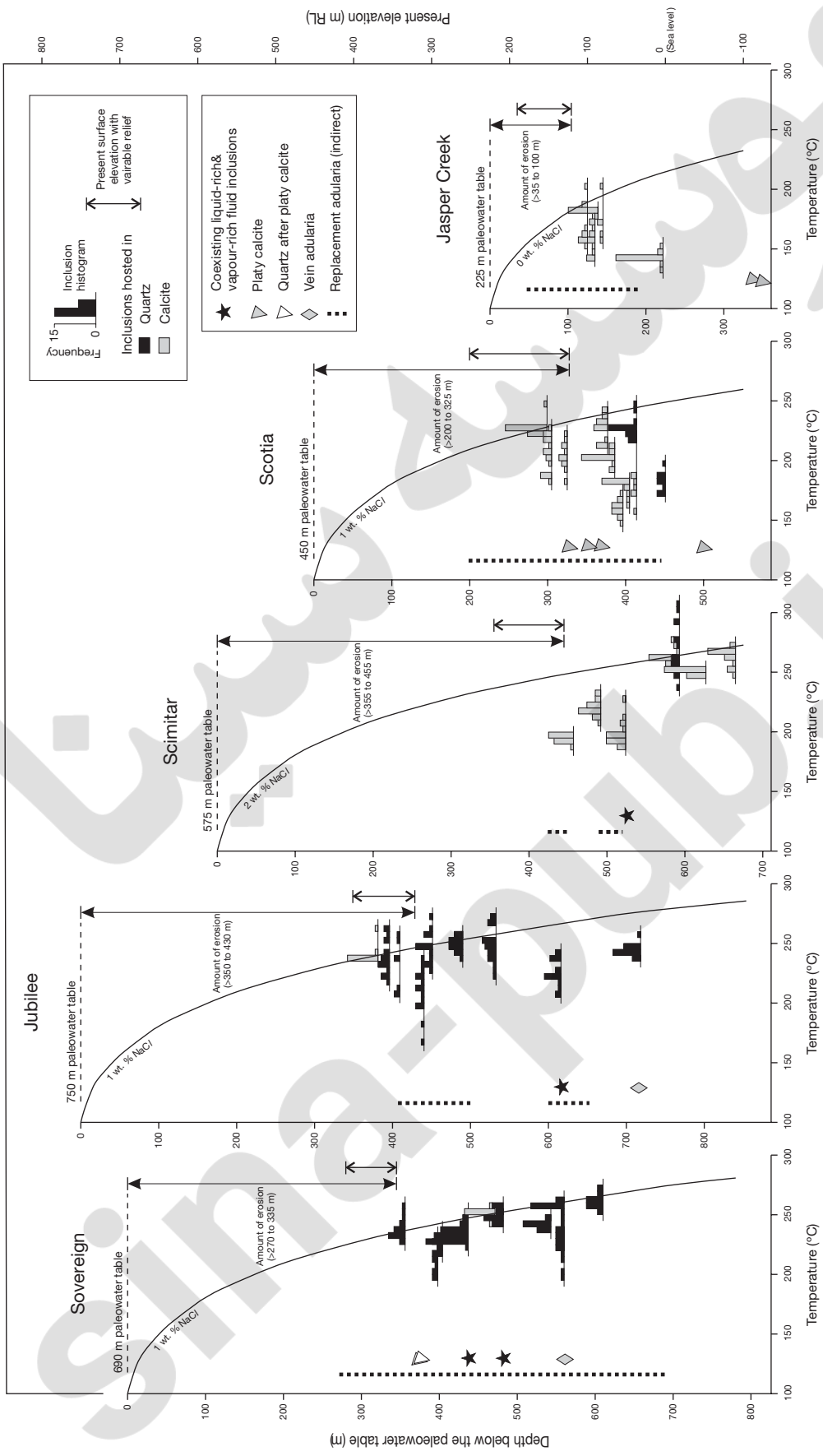

FIG. 17. Paleowater table positions estimated from fluid inclusion temperatures, apparent compositions, and relative to current elevations above the Sovereign, Jubilee, Scimitar, Scotia, and Jasper Creek deposits and prospects. The boiling point for depth curve at Sovereign is constrained by fluid inclusions trapped under boiling conditions. By contrast, the boiling point for depth curves for Jubilee, Scotia, and Jasper Creek are constrained by a single sample at each location, based on the highest T_h value (excluding obvious outliers), and assumes that these inclusions were trapped under near-boiling conditions. Some fluid inclusion histograms for Jubilee and Scotia show apparent lesser T_h values with depth; however, this is an artifact of data complication with samples covering a 400-m lateral extent and reflecting cooler temperatures to the east (cf. Fig. 14). Also shown are the depth occurrence of various minerals that form due to boiling fluids.

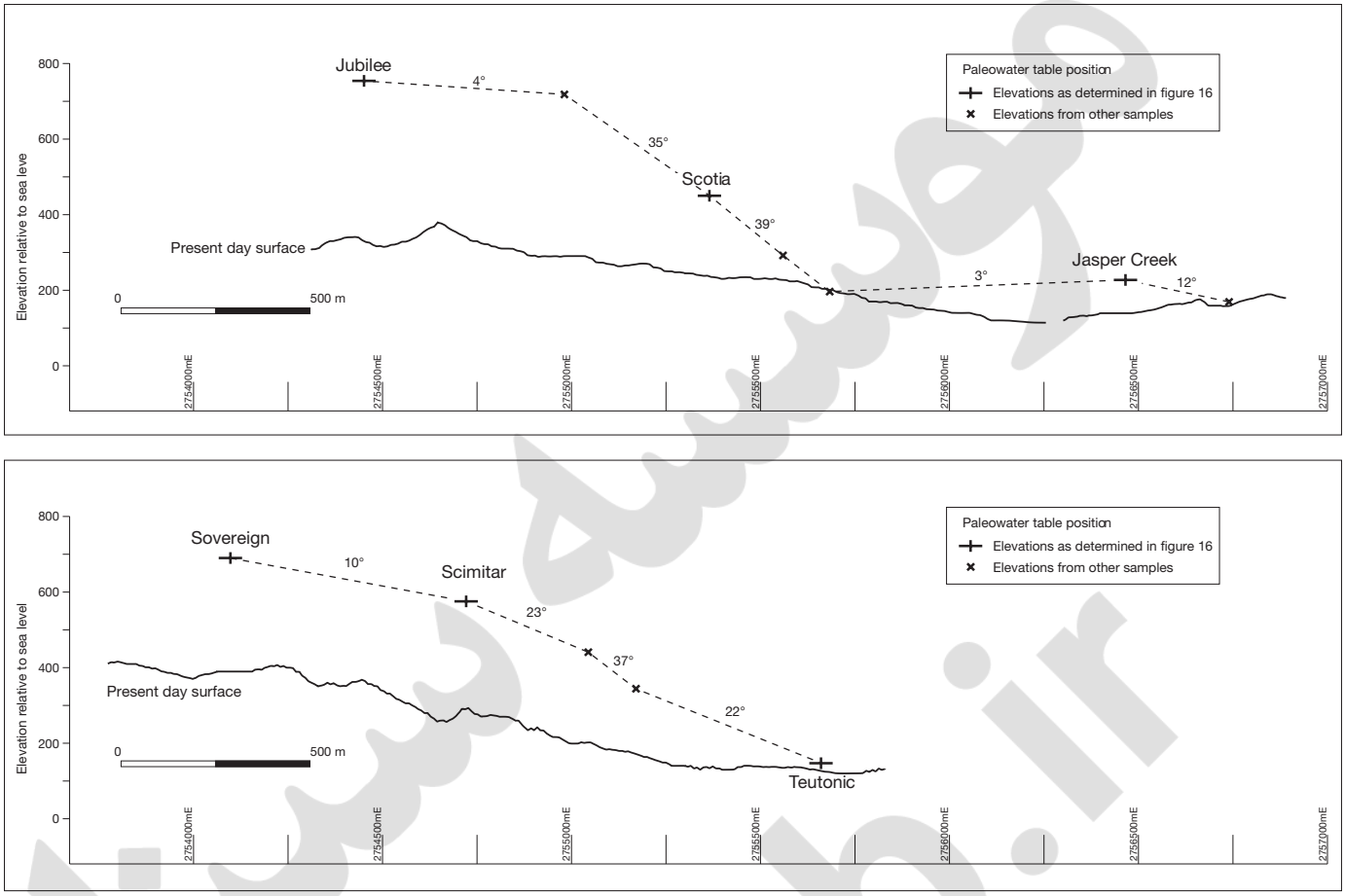

FIG. 18. Paleowater table elevations relative to current elevations, estimated for the Waitekauri area based on secondary fluid inclusions using the highest T_h and assuming trapping under boiling conditions. The paleowater table east of Jubilee, Sovereign, and west of Jasper Creek appears gently inclined (3°–10°), but in contrast is steeply dipping (36°–47°) east of Scimitar and at Scotia. The steep slope may indicate one or more faults with significant offset (>100 m).

The Waitekauri hydrothermal system

The Waitekauri deposits and prospects occur at the southern end of an irregularly shaped hydrothermal alteration zone that has demagnetized approximately 22 km² of rock, and encloses the Golden Cross, Maratoto, Komata, and Grace Darling deposits (Morrell et al., 2011; Fig. 2). Alteration of the host rocks at each deposit is broadly similar with the mineral association of quartz, adularia, chlorite, illite, interstratified illite-smectite, calcite, and pyrite (Main, 1979, Wayper, 1988; Simpson et al., 2001). The extent of the alteration zones surrounding individual deposits is poorly defined due to limited exposure, weathering, and local postmineral cover. Alteration surrounding veins at the Waitekauri deposits and prospects covers an area of approximately 3.5 km by 2.5 km (~7.5 km²).

High resolution $^{40}Ar/^{39}Ar$ dates of adularia from veins in the area have yielded preferred ages for many of the deposits in the region (Mauk et al., 2011). The Sovereign deposit yields a preferred age of 6.70 ± 0.16 Ma, which is younger then the preferred age of Golden Cross (6.98 ± 0.11 Ma), but older than those for Maratoto (6.41 ± 0.04 Ma) and Komata (6.06 ± 0.06 Ma; Mauk and Hall, 2004; Mauk et al., 2011). Perhaps these deposits formed in the same geothermal field with the locus of fluid flow migrating through time; however, the unique mineralogy at Waitekauri—with zeolites, epidote, and prehnite, which are not seen at the other deposits—suggests that the Waitekauri deposits and prospects likely formed in a smaller and separate geothermal field. Therefore, in the following discussion, we consider the Waitekauri hydrothermal system separately from the hydrothermal systems that formed other nearby deposits.

The interpreted thermal structure of the Waitekauri hydrothermal system, which is based on alteration minerals and fluid inclusion data, shows relatively high temperatures at Sovereign and Jubilee and relatively low temperatures at Teutonic and Jasper Creek (Fig. 19A). There are at least three possible hydrologic reconstructions that could account for this interpreted temperature gradient.

1. All the Waitekauri deposits and prospects formed in a single geothermal field with significant lateral outflow due to a hydraulic gradient caused by several hundred meters of vertical relief (Fig. 19B).

2. The deposits and prospects formed in a single low-relief geothermal field with an essentially flat-lying paleowater table that has subsequently been faulted and/or tilted by approximately 10° to 15°, resulting in greatest uplift and erosion to the west (Fig. 19C, D).

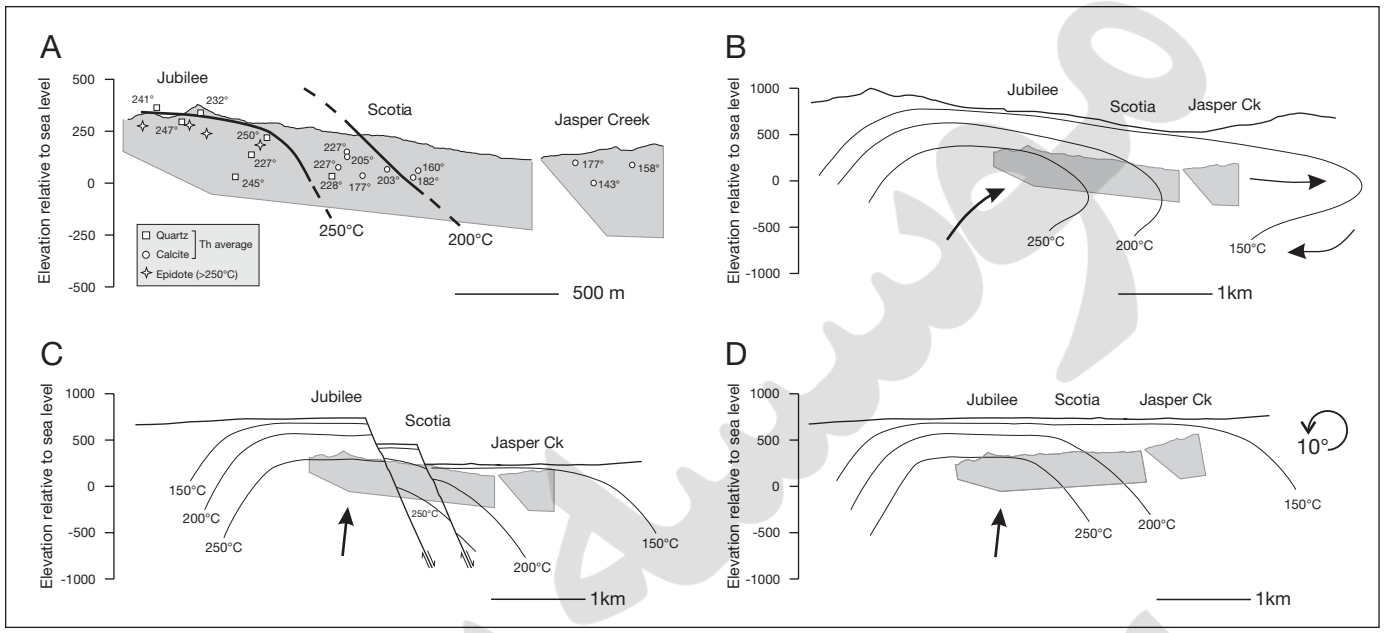

FIG. 19. Schematic diagram showing possible reconstructions of the Waitekauri hydrothermal system. A) Shows the Jubilee-Scotia-Jasper Creek cross section with temperature contours based on temperature-sensitive minerals and fluid inclusions. A similar thermal profile at Sovereign-Scimitar-Teutonic section is offset to the west and omitted for clarity. In B, C, and D, the temperature contours are extended beyond the known limits and are speculative. B) All deposits and prospects formed in a single geothermal field with significant lateral outflow to the east due to a hydraulic gradient caused by several hundred meters of vertical relief. C and D) A single low-relief geothermal field with an essentially flat-lying paleowater table that has subsequently been either faulted or tilted (~10°) after mineralization, respectively.

3. Alternatively, one or more of the Waitekauri deposits and prospects may have formed from separate geothermal fields. Although all three reconstructions could account for our results, the overall continuity of alteration mineralogy, changes in alteration intensity, and fluid inclusion results best supports the first two possibilities. Regardless of the preferred paleohydrologic reconstruction, the mineral association of quartz, adularia, albite, chlorite, illite, interstratified illite-smectite, smectite, calcite, and pyrite reflects formation from meteoric near-neutral pH chloride water with low concentrations of dissolved CO_2, with the highest paleotemperatures toward the west and lower paleotemperatures to the east. Changes in apparent fluid inclusion salinities suggest that fluids were more dilute to the east, and hematite may have formed from the mixing with more oxygenated marginal groundwaters. Late overprinting calcite alteration and calcite veins may have formed from descending CO_2-rich waters. Postmineral faulting or rotation subsequently produced greater erosion and deeper exposure of the prospects to the west.

Where is the gold?

The Jubilee vein has significant dimensions of 990 m × 215 m × 2.4 m, but produced only 13,700 oz of Au, and most of this came from a localized hanging-wall splay. This contrasts with the Favona vein, with similar dimensions of 1,000 m × 250 m × 1 to 3 m and a resource of >595,000 oz Au (Torckler et al., 2006; Simpson and Mauk, 2007), and the nearby Golden Cross deposits, where the Empire vein, with a smaller dimension of 500 × 250 m × 2 to 10 m wide, produced over 400,000 oz Au (Simpson et al., 2001; Begbie et al., 2007). Thus, although the Waitekauri deposits and prospects host significant veins, the area does not appear to be well endowed with Au. This apparent low Au endowment may reflect undiscovered resources not yet intersected by drilling or the removal of the resource by erosion. In the case of the latter, economic mineralization in epithermal deposits of the Hauraki goldfield and those globally generally are restricted over a vertical interval of ≤300 m; although some are exceptional with ≤600 m (Cooke and Simmons, 2000; Simmons et al., 2005; Christie et al., 2007). Moreover, at many epithermal deposits, economic mineralization is confined to a 200- to 300-m vertical interval, even though veins continue at depth below this economic zone (Simmons et al., 2005). Calculated formation depths at Waitekauri indicate that at least 300 to 400 m of material has been eroded above Jubilee and Sovereign and this eroded zone may have hosted the most intensely mineralized part of the vein system. Accordingly, Jubilee and Sovereign could represent the Au-poor roots of the vein system.

Alternatively, the apparent low Au endowment in the exposed portions of the Waitekauri area may simply reflect that this is a gold-poor system. Subeconomic concentrations of gold could be due to several factors including the following: (1) initial low concentrations of Au in the fluid, (2) host-rock rheologic controls, (3) conduit geometry, (4) fluid dilution, (5) temperature and/or (6) different combinations of the above (Simmons et al., 2005; Christie et al., 2007). For example, rheology coupled with conduit size and shape may have restricted gold deposition at Sovereign, because the main host

rock is a breccia and the veins are narrow and discontinuous (cf. Brathwaite et al., 2001b). At Jasper Creek, fluid dilution may have reduced metal solubility and suppressed Au deposition (e.g., Simmons and Browne, 2000).

Many of the above factors relate to the physical conditions of the gold "trap" but another fundamental control on the formation of an economic deposits is the Au-carrying capacity of the fluid. For example, the Taupo volcanic zone, New Zealand, contains both low and high gas geothermal fields where there is a close relationship between concentrations of CO_2, H_2S, and Au content; the CO_2 concentration also controls alteration mineralogy (calcite, zeolites, calc-silicates; Brown, 1986; Giggenbach, 1992, 1997; Brown and Simmons, 2003; Simmons and Brown, 2006, 2007). Geothermal fields with high levels of dissolved CO_2 and H_2S, and that have abundant calcite but lack zeolites can deposit ore-grade precipitates of Au and Ag on the back pressure plates of some geothermal wells (Weissberg, 1969; Brown, 1986; Krupp and Seward, 1987; Hedenquist, 1990). In contrast, geothermal fields with low CO_2 and H_2S concentrations, which have common zeolites, epidote, and little to no calcite, lack gold precipitates (Steiner, 1977; Rosenburg et al., 2009). Therefore, the occurrence of zeolites in the Waitekauri area may suggest that at least some veins formed from hydrothermal fluids with low gas and gold concentrations, and therefore the Au endowment at Waitekauri may originally have been low.

Conclusions

Drill core reveals spatial and temporal zonation of hydrothermal alteration and vein minerals along a 3-km-long composite cross section and a reconstructed 600-m vertical extent of epithermal adularia-sericite deposits and prospects in the Waitekauri area. Hydrothermal alteration is typically intense, although it becomes more variable and weaker toward the east; alteration and vein minerals show zoned distributions (this study), which is reflected by the geochemistry of the altered host rocks (Booden et al., 2011). Alteration minerals and fluid inclusion microthermometry suggest that the Sovereign and Jubilee deposits formed at relatively higher temperatures and at greater depth than the Jasper Creek prospect. Several reconstructions of the overall hydrothermal system are possible, but we infer that the Sovereign and Jubilee deposits formed in the main upflow area, whereas Jasper Creek formed toward the margin. The Waitekauri deposits and prospects may have formed in a single geothermal field with (1) significant lateral outflow to the east due to a hydraulic gradient imposed by several hundred meters of vertical relief or (2) in a single low-relief geothermal field with a flat-lying paleowater table that was faulted or tilted by 10° to 15° following mineralization. In either case, the greatest erosion (~300–400 m) has occurred at the Jubilee and Sovereign deposits and these may represent the roots of a more extensive vein network that has largely been eroded.

Acknowledgments

We thank Newmont Waihi Operations for providing access to the Waitekauri deposits and prospects, and for permission to publish. We thank Ross McConnochie, Rohan Worland, and Lorranace Torckler for geologic maps and for many insightful discussions. Kevin Faure of GNS Science is thanked for stable isotope analyses. Finally, we thank *Economic Geology* reviewers Peter Vikre, David John, and Jim Saunders for constructive reviews. This research has been funded by Newmont Waihi Operations and the New Zealand Foundation for Research Science and Technology (FRST).

REFERENCES

Adams, C.J., Graham, I.J., Seward, D., and Skinner, D.N.B., 1994, Geochronological and geochemical evolution of the late Cenozoic volcanism in the Coromandel peninsula, New Zealand: New Zealand Journal of Geology and Geophysics, v. 37, p. 359–379.

Begbie, M.J., Spörli, K.B., and Mauk, J.L., 2007, Structural evolution of the Golden Cross epithermal Au-Ag deposit, New Zealand: Economic Geology, v. 102, p. 873–892.

Bell, J.M., and Fraser, C., 1912, The Geology of the Waihi-Tairua subdivision, Hauraki, Auckland; New Zealand: New Zealand Geological Survey Bulletin, v. 15, 193p.

Bird, D.K., Schiffman, P., Elders, W.A., Williams, A.E., and McDowell, S.D., 1984, Calc-silicate mineralization in active geothermal systems: Economic Geology, v. 79, p. 671–695.

Bodnar, R.J., 1993, Revised equation and table for determining the freezing point depression of H_2O-NaCl solutions: Geochimica et Cosmochimica Acta, v. 57, p. 683–684.

Bodnar, R.J, Reynolds, T.J., and Kuehn, C.A., 1985, Fluid inclusions systematics in epithermal system: Reviews in Economic Geology, v. 2, p. 73–98.

Booden, M.A., Mauk, J.L., and Simpson, M.P., 2011, Quantifying metasomatism in epithermal Au-Ag deposits: A case study from the Waitekauri area, New Zealand: Economic Geology, v. 106, p. 999–1030.

Brathwaite, R.L., and Christie, A.B., 1996, Geology of the Waihi area, scale 1:50 000: Institute of Geological and Nuclear Sciences, Geological map 21, 1 sheet, 64 p.

Brathwaite, R.L., Simpson, M.P., Faure, K., and Skinner, D.N.B., 2001a, Telescoped porphyry Cu-Mo-Au mineralization, advanced argillic alteration and quartz-sulphide-gold-anhydrite veins in the Thames district, New Zealand: Mineralium Deposita, v. 36, p. 623-640.

Brathwaite, R.L., Cargill, H.J., Christie, A.B., and Swain, A., 2001b, Controls on the distribution of veining in andesite- and rhyolite- hosted gold-silver epithermal deposits of the Hauraki Goldfields, New Zealand: Mineralium Deposita, v. 36, p. 1–12.

Briggs, R.M., Houghton, B.F., McWilliams, M., and Wilson, C.N.J., 2005, $^{40}Ar/^{39}Ar$ ages of silicic volcanic rocks in the Tauranga-Kaimai area, New Zealand: Dating the transition between volcanism in the Coromandel arc and the Taupo volcanic zone: New Zealand Journal of Geology and Geophysics, v. 48, p. 459–469.

Brown, K.L., 1986, Gold deposition from geothermal discharges in New Zealand: Economic Geology, v. 81, p. 979–983.

Brown, K.L., and Simmons, S.F., 2003, Precious metals in high temperature geothermal systems in New Zealand: Geothermics, v. 32, p. 619–625.

Browne, P. R.L., 1978, Hydrothermal alteration in active geothermal fields: Annual Reviews in Earth and Planetary Sciences, v. 6, p. 229–250.

Browne, P.R.L., and Ellis, A.J., 1970, The Ohaki-Broadlands hydrothermal area, New Zealand: Mineralogy and related geochemistry: American Journal Science, v. 269, p. 97–131.

Browne, P.R.L., and Lawless, J. V., 2001, Characteristics of hydrothermal eruptions, with examples from New Zealand and elsewhere: Earth Science Reviews, v. 52, p. 299–331.

Christie, A.B., Simpson, M.P., Brathwaite, R.L., Mauk, J L., and Simmons, S.F., 2007, Epithermal Au-Ag and Related Deposits of the Hauraki Goldfield, Coromandel volcanic zone, New Zealand: Economic Geology, v. 102, 785–816.

Conrad, M.E., Petersen, U., and O'Neil, J.R., 1992, Evolution of an Au-Ag hydrothermal system: The Tayoltita mine, Durango, Mexico: Economic Geology, v. 87, p. 1451–1474.

Cooke, D.R., and Simmons, S.F., 2000, Characteristics and genesis of epithermal gold deposits: Reviews in Economic Geology, v. 13, p. 221–244.

de Ronde, C.E.J., and Blattner, P., 1988, Hydrothermal alteration, stable isotopes, and fluid inclusions of the Golden Cross epithermal gold deposit, Waihi, New Zealand: Economic Geology, v. 83, p. 895–917.

Downey, J.F., 1935, Gold mines of the Hauraki district: Wellington, New Zealand, Government Printer, 315 p.

Ellis, A.J., 1959, The solubility of calcite in carbon dioxide solutions: The American Journal of Science, v. 257, p. 354–365.
Essene, E.J. and Peacor, D.R., 1995, Clay mineral thermometry—a critical perspective: Clays and Clay Minerals, v. 43, p. 540–553.
Faure, K., and Brathwaite, R.L., 2006, Mineralogical and stable isotope studies of gold-arsenic mineralisation in the Sams Creek peralkaline porphyritic granite, South Island, New Zealand: Mineralium Deposita, v. 40, p. 802–827.
Friedman, I. and O'Neil, J.R., 1977, Compilation of stable isotope fractionation factors of geochemical interest: U.S. Geological Survey Prof. Paper 440-KK, 12 p.
Giggenbach, W.F., 1992, Magma degassing and mineral deposition in hydrothermal systems along convergent plate boundaries: Economic Geology, v. 87, p. 1927–1944.
——1997, The origin and evolution of fluids in magmatic-hydrothermal systems, *in* Barnes, H.L., ed., Geochemistry of hydrothermal ore deposits, 3rd ed.: New York, John Wiley and Sons, p. 737–796.
Grodzicki, K.R., Mauk, J.L., McConnochie, R., and Rowland, J.V., 2007, Structural geology of the Sovereign prospect, lower Waitekauri Valley, Hauraki goldfield, New Zealand: Proceedings of the 40th Annual Conference of the New Zealand Branch of the Australasian Institute of Mining and Metallurgy (AusIMM), p. 103–108.
Haas, J.L., 1971, The effects of salinity on the maximum thermal gradient of a hydrothermal system at hydrostatic pressure: Economic Geology, v. 66, p. 940–946.
Hartley, R.J., and McConnochie, M.R., 1991, Jubilee prospect, Waitekauri project PL 31-1777, Cyprus Gold NZ Ltd: Crown Minerals, Ministry of Economic Development, Wellington, unpublished open-file mineral report MR3043, 36 p.
Haworth, A.V., and Briggs, R.M., 2006, Epithermal Au-Ag mineralization in the Lower Waitekarui valley, Hauraki goldfield: Australasian Institute of Mining and Metallurgy (AusIMM) Monograph 25 p. 157–162.
Hedenquist, J.W., 1990, The thermal and geochemical structure of the Broadlands-Ohaaki geothermal system, New Zealand: Geothermics, v. 19, p. 151–185.
Hedenquist, J.W., and Browne, P.R.L., 1989, The evolution of the Waiotapu geothermal system, New Zealand, based on the chemical and isotopic composition of its fluids, minerals and rocks: Geochimica et Cosmochimica Acta, v. 53, p. 2235–2257.
Hedenquist, J.W., and Henley, R.W., 1985, Effect of CO_2 on freezing point depression measurements of fluid inclusions: Evidence from active systems and application to epithermal studies: Economic Geology, v. 80, p. 1379–1406.
Hedenquist, J.W., and Stewart, M.K., 1985, Natural CO_2-rich steam-heated waters at Broadlands, New Zealand: Their chemistry, distribution and corrosive nature: Proceedings Geothermal Resources Council Annual Meeting, Transactions, v. 9, p. 245–250.
Henley, R.W., and Ellis, A.J., 1983, Geothermal systems ancient and modern: A geochemical review: Earth Science Reviews, v. 19, p. 1–50.
Henley, R.H., and Hedenquist, J.W., 1986, Introduction to the geochemistry of active and fossil geothermal systems: Berlin-Stuttgart, Gerbruder Borntrager, Monograph Series Mineral Deposits, v. 26, p. 1–22.
Hoskin, P.W.O., Wysoczanski, R.J., and Briggs, R.M., 1998, U-Pb age determination of "Lenticulite" (Owharoa Ignimbrite) at Waikino, Waihi area, Coromandel peninsula, and implications [abs.]: Geological Society of New Zealand Miscellaneous Publication 101A, p. 123.
Houghton, B.F., Wilson, C.J.N., McWilliams, M.O., Lanphere, M.A., Weaver, S.D., Briggs, R.M., and Pringle, M.S., 1995, Chronology and dynamics of a large silicic magmatic system: central Taupo volcanic zone, New Zealand: Geology, v. 23, p. 13–16.
Hudson, D.M., 2003, Epithermal alteration and mineralization in the Comstock district, Nevada: Economic Geology, v. 98, p. 367–386.
Inoue, A., and Utada, M., 1983, Further investigations of a conversion series of dioctahedral mica/smectites in the Shinzan hydrothermal alteration area, northeast Japan: Clays and Clay Minerals, v. 31, p. 401–412.
John, D.A., Hofstra, A. H., Fleck, R.J., Brummer, J.E., and Saderholm, E.C., 2003, Geologic setting and genesis of the Mule Canyon low-sulfidation epithermal gold-silver deposit, north-central Nevada: Economic Geology, v. 98, p. 425–464.
Krupp, R.E., and Seward, T.M., 1987, The Rotokawa geothermal system, New Zealand: An active epithermal gold-depositing environment: Economic Geology, v. 82, p. 1109–1129.
Main, J.V., 1979, Precious metal bearing veins of the Maratoto-Wentworth area, Hauraki goldfield, New Zealand: New Zealand Journal of Geology and Geophysics, v. 22, p. 41–51.
Mas, A., Guisseau, D., Patrier Mas, P., Beaufort, D., Genter, A., Sanjuan, B., and Girard, J. P., 2006, Clay minerals related to the hydrothermal activity of the Bouillante geothermal field (Guadeloupe): Journal of Volcanology and Geothermal Research, v. 158, p. 380–400.
Matsuhisa, Y., Goldsmith, J.R., and Clayton, R.N., 1979, Oxygen isotopic fractionation in the system quartz-albite-anorthite-water: Geochimica et Cosmochimica Acta, v. 43, p. 1131–1140.
Mauk, J.L., and Hall, C.M., 2004, $^{40}Ar/^{39}Ar$ ages of adularia from Golden Cross, Neavesville, and Komata epithermal deposits, Hauraki goldfield, New Zealand: New Zealand Journal of Geology and Geophysics, v. 47, p. 227–231.
Mauk, J.L., Hall, C.M, Chesley, J.T., and Barra, F., 2011, Punctuated evolution of a large epithermal province: The Hauraki goldfield, New Zealand: Economic Geology, v. 106, p. 921–943.
McOnie, A., 2001, Waitekauri project—progress report, exploration permit 40 344, year ending March 2001, Coeur Gold New Zealand Ltd: Crown Minerals, Ministry of Economic Development, Wellington, unpublished open-file mineral report MR3874, 15 p.
Moore, D.M., and Reynolds, R.C., 1997, XRD and the identification and analysis of clay minerals (second edition): Oxford University Press, 378 p.
Morrell, A.E., Locke, C.A., Cassidy, J., Mauk, J.L., 2011, Geophysical characteristics of adularia-sericite epithermal gold-silver deposits in the Waihi-Waitekauri region, New Zealand: Economic Geology, v. 106, p. 1031–1041.
Mortimer, N., Herzer, R.H., Gans, P.B., Laporte-Magoni, C., Calvert, A.T., and Bosch, D., 2007, Oligocene-Miocene tectonic evolution of the South Fiji basin and Northland Plateau, SW Pacific Ocean: Evidence from petrology and dating of dredged rocks: Marine Geology, v. 237, p. 1–24.
Nicholson, K.N., Black, P.M., Hoskin, P.W.O., and Smith, I.E.M., 2004, Silicic volcanism and back-arc extension related to migration of the late Cainozoic Australian-Pacific plate boundary: Journal of Volcanology and Geothermal Research, v. 131, p. 295–306.
Okada, H., Yasudaa, Y., Yagi, M., and Kaia, K., 2000, Geology and fluid chemistry of the Fushime geothermal field, Kyushu, Japan: Geothermics, v. 29, p. 279–311.
Reyes, A.G., 1990, Petrology of Philippine geothermal systems and the application of alteration mineralogy to their assessment; Journal of Volcanology and Geothermal Research, v. 43, p. 279–309.
Reynolds, R.C., 1980, Interstratified clay minerals, *in* Brindley, G,W., and Brown, G., eds., Crystal structures of clay minerals and their X-ray identification: Mineralogical Society of London, p. 249–303.
Roedder, E., 1984, Fluid inclusions: Reviews in Mineralogy, v. 12, 644 p.
Rosenburg, M.D., Bignall, G., and Rae, A.J., 2009, The geological framework of the Wairakei-Tauhara geothermal system, New Zealand: Geothermics, v. 38, p. 72–84.
Seward, T.M., and Barnes, H.L., 1997, Metal transport by hydrothermal fluids, *in* Barnes, H.L., ed., Geochemistry of hydrothermal ore deposits, 3rd edition: John Wiley and Sons, Inc, p. 435–486.
Simmons, S.F., and Brown, K.L., 2006, Gold in magmatic hydrothermal solutions and the rapid formation of a giant ore deposit: Nature, v. 314, p. 288–291.
——2007, The flux of gold and related metals through a volcanic arc, Taupo volcanic zone, New Zealand: Geology, v. 35, p. 1099–1102.
Simmons, S.F., and Browne, P.R.L., 2000, Hydrothermal minerals and precious metals in the Broadlands-Ohaaki geothermal system: Implications for understanding low-sulfidation epithermal environments: Economic Geology, v. 95, p. 971–1000.
Simmons, S.F., and Christenson, B.W., 1994, Origins of calcite in a boiling geothermal system: American Journal Science, v. 294, p. 361–400.
Simmons, S.F., Arehart, G., Simpson, M.P., Mauk, J.L., 2000, Origin of massive calcite veins in the Golden Cross, low-sulfidation epithermal Au-Ag deposit, New Zealand, Economic Geology, v. 95, p. 99–112.
Simmons, S.F., White, N.C., and John, D., 2005, Geological characteristics of epithermal precious and base metal deposits: Economic Geology 100th Anniversary Volume, p. 485–522.
Simpson, C.R.J., Mauk, J.L., and Arehart, G., 1995, The formation of banded epithermal quartz veins at the Golden Cross mine, Waihi, New Zealand: Australasian Institute of Mining and Metallurgy, Pacrim Congress 1995, Auckland, New Zealand, Nov. 19–22, p. 545–550.
Simpson, M.P., and Mauk, J.L., 2007, The Favona epithermal gold-silver deposit, Waihi, New Zealand: Hydrothermal alteration, hydrologic evolution and implications for exploration: Economic Geology, v. 102, p. 817–839.

Simpson, M.P., Simmons, S.F., and Mauk, J.L., 2001, Hydrothermal alteration and hydrologic evolution of the Golden Cross epithermal Au-Ag deposit, New Zealand: Economic Geology, v. 96, p. 773–796.
Skinner, D.N.B., 1986, Neogene volcanism of the Hauraki volcanic region: Royal Society of New Zealand Bulletin, v. 23, p. 20–47.
——1995, Geology of the Mercury Bay area: Institute of Geological and Nuclear Sciences geological map 17, scale 1:50,000, 1 sheet, 56 p.
Steiner, A., 1968, Clay minerals in hydrothermally altered rocks at Wairakei, New Zealand: Clays and Clay Minerals, v. 16, p. 193–213.
——1977, The Wairakei geothermal area, North Island, New Zealand: New Zealand Geological Survey Bulletin, 90, 136 p.
Sterner, S.M., 1992, Homogenization of fluid inclusions to the vapor phase: The apparent homogenization phenomenon: Economic Geology, v. 87, p. 1616–1623.
Tillick, D.A., Peacor, D.R., Mauk, J.L., and Peacor, D.R., 2001, Genesis of dioctahedral phyllosilicates during hydrothermal alteration of volcanic rocks: 1. The Golden Cross epithermal ore deposit, New Zealand: Clays and Clay Minerals, v. 49, p. 126–140.
Torckler, L.K., McKay, D., and Hobbins, J., 2006, Geology and exploration of the Favona Au-Ag deposit, Waihi, Hauraki goldfield: Australasian Institute of Mining and Metallurgy Monograph 25 p. 179–184.
Vaughan, D.J., and Craig, J.R., 1997, Sulfide ore mineral stability, morphologies, and intergowth textures, *in* Barnes, H.L., ed., Geochemistry of hydrothermal ore deposits, 3rd edition: John Wiley and Sons, Inc, p. 367–434.
Watanabe, T., 1981, Identification of illite/montmorillonite interstratifications by X-ray diffraction: Journal Mineralogical Society Japan, Special Issue, v. 15, 32–41. (in Japanese)
Wayper, R.Y., 1988, Petrology of the Komata gold-silver epithermal ore deposit, Coromandel peninsula, New Zealand: Unpublished M.Sc. thesis, Wellington, Victoria, University of Wellington, 152 p.
Weissberg, B.G, 1969, Gold-silver ore-grade precipitates from New Zealand thermal waters: Economic Geology, v. 64, p. 95–108.
White, D.E., 1955, Thermal springs and epithermal ore deposits: Economic Geology 50th Anniversary Volume, p. 99–154.
——1981, Active geothermal systems and hydrothermal ore deposits: Economic Geology 75th Anniversary Volume, p. 392–423.
White, P.D., 1991, Progress report on Scotia prospect PL 31-1777, Waitekauri Valley: Cyprus Gold NZ Ltd. Crown Minerals, Ministry of Economic Development, Wellington, unpublished open-file mineral report MR3051, 34 p.